Acta Mech 229, 2495–2519 (2018)
https://doi.org/10.1007/s00707-018-2113-7

ORIGINAL PAPER

Wei Tong

Calibration of a complete homogeneous polynomial yield function of six degrees for modeling orthotropic steel sheets

Received: 5 June 2017 / Revised: 19 September 2017 / Published online: 8 February 2018

Abstract For better modeling plane-stress anisotropic plasticity of steel sheets, a direct calibration method is proposed and detailed for establishing a positive and convex sixth-order homogeneous polynomial yield function with up to sixteen independent material constants. The calibration method incorporates parameter identification, convexity testing, and if needed, an adjustment of an initially calibrated but non-convex yield function toward a convex one. Some advantages of the calibration method include (i) a systematic solution of only linear equations for the sixteen material constants of a steel sheet with various degrees of planar anisotropy, (ii) a practical numerical implementation of the necessary and sufficient conditions for convexity certification of the calibrated or adjusted yield function, and (iii) an incremental procedure using a parameterized version of the initially calibrated and non-convex yield function that can always lead to an approximate sixth-order yield function with guaranteed convexity. Results of applying the proposed calibration method to successfully obtain convex sixth-order yield functions are presented for three steel sheets with experimental measurement inputs from various types and numbers per type of uniaxial and biaxial tension tests.

List of symbols

x, y, z	The orthotropic material symmetry axes corresponding to the rolling (RD), transverse (TD), and normal (ND) directions of a thin sheet metal
$\sigma_x, \sigma_y, \tau_{xy}$	Three in-plane Cartesian (two normal and one shear) components of an applied Cauchy stress $\boldsymbol{\sigma}$ in the orthotropic coordinate system of the sheet metal
$\Phi_2, A_1,\ldots, A_4$	Hill's 1948 quadratic anisotropic yield function [9] in plane stress and its four material constants
$\Phi_4, A_1,\ldots, A_9$	Gotoh's 1977 fourth-order anisotropic yield function [6] in Cartesian stress components $(\sigma_x, \sigma_y, \tau_{xy})$ and its nine material constants
$\Phi_6, A_1,\ldots, A_{16}$	The sixth-order homogeneous polynomial anisotropic yield function in Cartesian stress components $(\sigma_x, \sigma_y, \tau_{xy})$ and its sixteen material constants
$\sigma_1, \sigma_2, \theta$	The so-called intrinsic variables of an applied plane stress $\boldsymbol{\sigma}$ according to Hill [12,13], namely, the in-plane principal stresses (σ_1, σ_2) and the loading orientation angle θ between $\sigma_1 (\geq \sigma_2)$ and the rolling direction of the sheet metal

W. Tong (✉)
Department of Mechanical Engineering, Lyle School of Engineering, Southern Methodist University, Dallas, TX 75275-0337, USA
E-mail: wtong@lyle.smu.edu
Tel.: +(214)-768-1269
Fax: +(214)-768-1473

$\sigma_\theta, r_\theta, \sigma_b, r_b$	Yield stresses and plastic strain ratios under uniaxial tension ($\sigma_1 = \sigma_\theta > 0, \sigma_2 = 0$) at the loading orientation angle θ; and yield stress and plastic strain ratio under equal biaxial tension ($\sigma_1 = \sigma_2 = \sigma_b > 0$)
$\sigma_{p\theta}, \sigma_{s\theta}$	Yield stresses under near plane-strain tension ($\sigma_1 = 2\sigma_2 = \sigma_{p\theta} > 0$) and under pure shear stress ($\sigma_1 = -\sigma_2 = \sigma_{s\theta} > 0$) at the loading orientation angle θ
$\phi_6, F(\theta), G(\theta), H(\theta), N(\theta)$	The sixth-order yield function recast in intrinsic variables in a compact form of seven homogeneous principal stress terms and its four in-plane anisotropic functions. $F_0,\ldots,F_6$, and so forth are the 25 nonzero Fourier cosine series coefficients of those four functions
$\Psi_{6A}, \Psi_{6B}, \Psi_{6C}$	Three sub-determinants or leading principal minors of the Hessian matrix of the sixth-order yield function Φ_6 in Cartesian stress components ($\sigma_x, \sigma_y, \tau_{xy}$)
$\psi_{6A}, \psi_{6B}, \psi_{6C}$	Three sub-determinants $\Psi_{6A}, \Psi_{6B}, \Psi_{6C}$ of the Hessian matrix of the sixth-order yield function Φ_6 recast in intrinsic variables ($\sigma_1, \sigma_2, \theta$)
ρ, ω	The polar coordinates for the two principal stresses σ_1 and σ_2

1 Introduction

In the final Chapter of his classical monograph on mathematical plasticity, Hill [10] suggested that "for the yield function and plastic potential a polynomial of degree of n in the reduced stress components" takes the following form for an orthotropic sheet metal under a state of plane stress:

$$P_n(\sigma_x, \sigma_y, \tau_{xy}) = f^n(\boldsymbol{\sigma}) = \sum A_{ijk}\sigma_x^i\sigma_y^j\tau_{xy}^k \tag{1}$$

where $\boldsymbol{\sigma} = (\sigma_x, \sigma_y, \tau_{xy})$ is the applied Cauchy stress with its Cartesian components in sheet metal orthotropic axes (with the x-axis and y-axis being corresponding to the rolling and transverse directions of a sheet metal), the stress exponents i, j, k are positive integers or zero with $i + j + k \le n$ and k must be even, and $f(\boldsymbol{\sigma})$ is the equivalent yield stress used to define the yield criterion in terms of the yield strength σ_f of the sheet metal as $f(\boldsymbol{\sigma}) - \sigma_f = 0$. The simplest case of *homogeneous* polynomials in the above form (i.e., $i + j + k = n$) is the well-known quadratic yield function by Hill [9] with $n = 2$ and $k = 0$ or 2,

$$\Phi_2(\sigma_x, \sigma_y, \tau_{xy}) = A_1\sigma_x^2 + A_2\sigma_x\sigma_y + A_3\sigma_y^2 + A_4\tau_{xy}^2, \tag{2}$$

where A_1, A_2, A_3, and A_4 are its four non-dimensional material constants that are often determined using yield stress and plastic strain ratio measurements from two on-axis and one off-axis uniaxial tension tests, see [16].

In recent years, non-quadratic homogeneous polynomials are increasingly being used as yield functions to overcome the limitations or deficiencies of Hill's 1948 quadratic yield function. For example, Gotoh [6] proposed in 1977 the use of a plane stress fourth-order homogeneous polynomial yield function with orthotropic symmetry, namely ($i + j + k = 4$ and $k = 0, 2$ or 4 per Eq. (1)):

$$\begin{aligned}\Phi_4(\sigma_x, \sigma_y, \tau_{xy}) = {} & A_1\sigma_x^4 + A_2\sigma_x^3\sigma_y + A_3\sigma_x^2\sigma_y^2 + A_4\sigma_x\sigma_y^3 + A_5\sigma_y^4 \\ & + A_6\sigma_x^2\tau_{xy}^2 + A_7\sigma_x\sigma_y\tau_{xy}^2 + A_8\sigma_y^2\tau_{xy}^2 + A_9\tau_{xy}^4\end{aligned} \tag{3}$$

where A_1, A_2,… and A_9 are its nine non-dimensional material constants. As suggested by Gotoh [6], a set of nine linear equations using one measurement of yield stress σ_b from an equal biaxial tension test and eight measurements in yield stresses and plastic strain ratios (σ_0, σ_{45}, σ_{90}, σ_θ, r_0, r_{45}, r_{90}, r_θ, where $\theta = 22.5°$ or $67.5°$)[1] from four uniaxial tension tests may be used to uniquely determine these nine material constants. Two examples of the calibrated fourth-order yield function were also given by Gotoh [7]: one for a commercial Al-killed steel and another for a 1/4H copper alloy.

Empirical evidences have shown that an even higher-order yield function may be needed for more accurately modeling isotropic and anisotropic plasticity of metals [5,8,14,15,18,29]. For many BCC steel sheets, a sixth-order yield function is often preferred for its higher flexibility [3,27,30]. Such a choice has also been justified in

[1] Here the numerical subscript of the yield stress σ and plastic strain ratio r is the angle θ in degrees between the uniaxial tensile loading axis and the rolling direction of a sheet metal.

part based on the results by Logan and Hosford [19] that a yield function in the form of $\sigma_x^6 + \sigma_y^6 + (\sigma_x - \sigma_y)^6$ approximates closely the calculated upper bound yield loci of randomly oriented BCC polycrystals with <111>-pencil glide. As shown by Soare et al. [22] and Yoshida et al. [30], a complete homogeneous polynomial yield function of six degrees has the following form ($i + j + k = 6$ and $k = 0, 2, 4$ or 6 per Eq. (1)):

$$\begin{aligned}\Phi_6 = {} & A_1\sigma_x^6 + A_2\sigma_x^5\sigma_y + A_3\sigma_x^4\sigma_y^2 + A_4\sigma_x^3\sigma_y^3 + A_5\sigma_x^2\sigma_y^4 + A_6\sigma_x\sigma_y^5 \\ & + A_7\sigma_y^6 + A_8\sigma_x^4\tau_{xy}^2 + A_9\sigma_x^3\sigma_y\tau_{xy}^2 + A_{10}\sigma_x^2\sigma_y^2\tau_{xy}^2 + A_{11}\sigma_x\sigma_y^3\tau_{xy}^2 \\ & + A_{12}\sigma_y^4\tau_{xy}^2 + A_{13}\sigma_x^2\tau_{xy}^4 + A_{14}\sigma_x\sigma_y\tau_{xy}^4 + A_{15}\sigma_y^2\tau_{xy}^4 + A_{16}\tau_{xy}^6\end{aligned} \tag{4}$$

where A_1, A_2,… and A_{16} are its non-dimensional material constants to be determined by using sixteen experimental measurements from some simple mechanical tests. However, such a complete homogeneous polynomial yield function with its set of sixteen independent material constants has rarely if ever been fully calibrated to model a steel sheet subjected to biaxial or tri-component plane stress loading. Instead, the vast majority of steel sheet forming applications appearing in the literature have used only one of *reduced* sixth-order yield functions based on linearly transformed stresses [3,30]. These reduced yield functions with a much smaller number of independent material constants do not however utilize the full potential of a sixth-order yield function for modeling the directional and multi-axial dependence of the yielding and plastic flow of an anisotropic steel sheet.

There is mainly a twofold reason for such a situation. First, experimental measurements with a total of the required sixteen yield stresses and plastic strain ratios under uniaxial and biaxial loading are simply not commonly available for a steel sheet due to the complexity and/or cost of the material testing. Interestingly, unlike the case of Gotoh's fourth-order yield function of Eq. (3), there appears not to have been many detailed investigations similar to the ones presented by Gotoh [6,7] at all about the required types and numbers per type of measurements from simple mechanical tests of sheet metal samples that will constitute a set of sixteen independent inputs for fully calibrating all material constants of the sixth-order yield function of Eq. (4). Secondly and maybe more important, even if such a set of experimental input data is made available and all material constants are identified accordingly by solving a set of sixteen linear algebraic equations, the positivity and especially convexity of the calibrated yield function are both unknown and not guaranteed.

In fact, the second point above applies to any polynomial yield function of Eq. (1) so some additional restrictions on the material constants in a polynomial yield function have to be imposed to ensure it being positive and convex [11,13]. Hill's 1948 quadratic yield function of Eq. (2) is a rather special case. The necessary and sufficient conditions for it to be strictly positive and convex are the same and they are given by the following simple algebraic inequalities or restrictions on its four material constants:

$$A_1 > 0, \quad A_3 > 0, \quad A_4 > 0, \quad 4A_1A_3 > A_2^2. \tag{5}$$

For a non-quadratic plane stress polynomial yield function such as Φ_4 or Φ_6, however, such a complete set of simple algebraic relations on their material constants that can serve as the necessary and sufficient conditions on its positivity and convexity have not been reported so far in the open literature. It is noted that Gotoh in his original work did not address the important mathematical issue of positivity and convexity about his yield function at all. That is, Gotoh [7] only implicitly assumed but never explicitly established the positivity and convexity of his fourth-order yield function calibrated for the Al-killed steel and 1/4H copper sheets. Recently, there was an effort of developing positive and convex polynomial yield functions of four, six, and eight degrees by a nonlinear optimization numerical technique with additional constraints [22]. In particular, it included some positivity and convexity restrictions at some representative plane stress states as part of the optimized parameter identification scheme to increase the likelihood of a resulting yield function being positive and convex over the entire plane stress space and to fill the gap of missing experimental inputs. As pointed out by Yoshida et al. [30], such an approach seemed to be working practically "but theoretically still it is not perfect." In other words, the positivity and convexity constraints used in their parameter identification technique are only necessary but not sufficient. The resulting yield function is still not guaranteed to be positive and convex over plane stress states other than the ones used in the optimization.

In this study, we present an alternative method of directly calibrating and establishing a positive and convex polynomial yield function of six degrees with up to sixteen independent material constants for steel sheets. The proposed calibration method consists of three components: (i) transformation of the yield function Φ_6 into a form in terms of the intrinsic stress variables and parameter identification of its 16 independent Fourier coefficients by solving a set of linear equations using various types and numbers per type of experimental

measurements from simple mechanical tests; (ii) convexity testing of the calibrated sixth-order yield function via a practical numerical implementation of the necessary and sufficient conditions; and (iii) incremental parameter adjustments of the as-calibrated but non-convex yield function that can always lead to an approximate yield function with guaranteed convexity. These three key components of the calibration method were recently proposed by Tong [23–25], and they have been successfully applied to obtain positive and convex Gotoh's fourth-order yield functions for many sheet metals [26].

In the following several Sections, we describe one-by-one the details of each component of the new calibration method being extended to the sixth-order yield function. Numerous examples are given in a mechanically meaningful and mathematically consistent way on how to calibrate a sixth-order yield function with either full planar anisotropy or various degrees of reduced planar anisotropy using a number of independent experimental measurements anywhere between 1 and 16. In Sect. 6, we present numerical results of the new calibration method being applied to model three selected steel sheets by the sixth-order yield function using all 13, 11, and 10 available and independent experimental inputs, respectively. Not only all five individual cases of the sixth-order yield function calibrated for the three steels were verified to be strictly positive and convex, but the convexity limit was also estimated for each calibrated yield function using a single scalar variable. Possible further improvements of the proposed calibration method for constructing a convex sixth-order polynomial yield function were also briefly discussed, and some conclusions drawn from the current study are given in Sect. 7.

2 The sixth-order yield function in terms of intrinsic variables

To facilitate the investigation about various types and numbers per type of measurements from simple mechanical tests that are required to fully calibrate the sixteen independent material constants of a sixth-order yield function $\Phi_6(\sigma_x, \sigma_y, \tau_{xy})$, we first reformulate the yield function in terms of intrinsic variables $(\sigma_1, \sigma_2, \theta)$ of an applied plane stress.[2] By using the standard plane stress coordinate transformation formulas

$$\sigma_x = \sigma_1 \cos^2\theta + \sigma_2 \sin^2\theta, \quad \sigma_y = \sigma_1 \sin^2\theta + \sigma_2 \cos^2\theta, \quad \tau_{xy} = (\sigma_1 - \sigma_2)\sin\theta\cos\theta \tag{6}$$

one can rewrite the sixth-order yield function of Eq. (4) in a compact form in terms of seven homogeneous principal stress terms, namely

$$\begin{aligned} \phi_6(\sigma_1, \sigma_2, \theta) = {} & F(\theta)\sigma_1^6 + G(\theta)\sigma_1^5\sigma_2 + H(\theta)\sigma_1^4\sigma_2^2 + N(\theta)\sigma_1^3\sigma_2^3 \\ & + H\left(\theta + \frac{\pi}{2}\right)\sigma_1^2\sigma_2^4 + G\left(\theta + \frac{\pi}{2}\right)\sigma_1\sigma_2^5 + F\left(\theta + \frac{\pi}{2}\right)\sigma_2^6, \end{aligned} \tag{7}$$

where the four functions $F(\theta)$, $G(\theta)$, $H(\theta)$, and $N(\theta)$ can be expressed in the Fourier cosine series form as

$$\begin{aligned} F(\theta) &= F_0 + F_1\cos 2\theta + F_2\cos 4\theta + F_3\cos 6\theta + F_4\cos 8\theta + F_5\cos 10\theta + F_6\cos 12\theta, \\ G(\theta) &= G_0 + G_1\cos 2\theta + G_2\cos 4\theta + G_3\cos 6\theta + G_4\cos 8\theta + G_5\cos 10\theta + G_6\cos 12\theta, \\ H(\theta) &= H_0 + H_1\cos 2\theta + H_2\cos 4\theta + H_3\cos 6\theta + H_4\cos 8\theta + H_5\cos 10\theta + H_6\cos 12\theta, \\ N(\theta) &= N_0 + N_2\cos 4\theta + N_4\cos 8\theta + N_6\cos 12\theta, \end{aligned} \tag{8}$$

and their 25 nonzero coefficients $F_0, F_1, \ldots, N_6$ are linear combinations of the 16 material constants $A_1, \ldots, A_{16}$ (see "Appendix A" for details). As expected, the yield function has the required symmetry properties of an orthotropic yield function in intrinsic variables as discussed by Hill [13]. Obviously, there are only up to 16 independent Fourier coefficients in these four anisotropic functions as well. One can use the linear algebra analysis to systematically check and identify both independent and non-independent ones. There will be many choices of 16 independent Fourier coefficients, and we adapt a general rule to choose as many independent coefficients as possible in the order of four functions $F(\theta)$, $G(\theta)$, $H(\theta)$, and $N(\theta)$. One such selection is $(F_0, F_1, F_2, F_3, F_4, F_5, F_6, G_0, G_1, G_2, G_3, G_4, H_0, H_1, N_0, N_2)$, and other nine coefficients are linear combinations of these sixteen coefficients, namely

$$\begin{aligned} &G_5 = -4F_5, \quad G_6 = -6F_6, \quad H_2 = -F_2 - G_2 - \frac{1}{2}N_2, \quad H_3 = -3F_3 - 2G_3, \\ &H_4 = -9F_4 - 4G_4, \quad H_5 = 5F_5, \quad H_6 = 15F_6, \quad N_4 = 16F_4 + 6G_4, \quad N_6 = -20F_6. \end{aligned} \tag{9}$$

[2] Here σ_1 and σ_2 are principal stresses, and θ is the in-plane angle between the axis of the principal stress $\sigma_1 (\geq \sigma_2)$ and the x-axis of the material symmetry axes (i.e., the rolling direction of a sheet metal). They are called intrinsic variables of the applied stress by Hill [12,13].

As the plastic axial strain increments in the two principal stress axes are given by $\dot{\varepsilon}_1^p \propto \partial\phi_6/\partial\sigma_1$ and $\dot{\varepsilon}_2^p \propto \partial\phi_6/\partial\sigma_2$ per the associated flow rule ([12,13]), one can show that the plastic strain ratio under uniaxial tension at a loading orientation angle θ is given as (with $\sigma_1 = \sigma_\theta > 0$, $\sigma_2 = 0$ and plastic incompressibility is assumed as usual for metals)

$$\begin{aligned} r_\theta =& \frac{\dot{\varepsilon}_2^p}{\dot{\varepsilon}_3^p} = -\frac{\dot{\varepsilon}_2^p}{\dot{\varepsilon}_1^p + \dot{\varepsilon}_2^p} = -\frac{G(\theta)}{6F(\theta) + G(\theta)} \\ =& \frac{-G_0 - G_1\cos2\theta - G_2\cos4\theta - G_3\cos6\theta - G_4\cos8\theta + 4F_5\cos10\theta + 6F_6\cos12\theta}{6F_0 + G_0 + (6F_1 + G_1)\cos2\theta + (6F_2 + G_2)\cos4\theta + (6F_3 + G_3)\cos6\theta + (6F_4 + G_4)\cos8\theta + 2F_5\cos10\theta}. \end{aligned} \tag{10}$$

Similarly, the plastic strain ratio under equal or balanced biaxial tension r_b is given as (with $\sigma_1 = \sigma_2 = \sigma_b > 0$, $\theta = 0$)

$$r_b = \frac{\dot{\varepsilon}_2^p}{\dot{\varepsilon}_1^p} = \frac{6F_0 - 6F_1 + 6G_0 - 4G_1 + 6H_0 - 2H_1 + 3N_0}{6F_0 + 6F_1 + 6G_0 + 4G_1 + 6H_0 + 2H_1 + 3N_0}. \tag{11}$$

For a general plane stress state with $\sigma_1 > 0$ and the yield condition $\phi_6(\boldsymbol{\sigma}) - \sigma_f^6 = 0$, Eq. (7) may be rewritten as

$$\left(\frac{\sigma_f}{\sigma_1}\right)^6 = F(\theta) + \zeta G(\theta) + \zeta^2 H(\theta) + \zeta^3 N(\theta) + \zeta^4 H\left(\theta + \frac{\pi}{2}\right) + \zeta^5 G\left(\theta + \frac{\pi}{2}\right) + \zeta^6 F\left(\theta + \frac{\pi}{2}\right) \tag{12}$$

where $\zeta = \sigma_2/\sigma_1$ is the biaxial plane stress ratio between -1 and 1. Some common plane stress states can be specified accordingly: $\zeta = 0$ for uniaxial tension; $\zeta = 1$ for equal biaxial tension; $\zeta = -1$ for pure shear stress; $\zeta = 1/2$ for near or approximate plane-strain tension. The yield stress under uniaxial tension σ_θ at a loading orientation angle θ is thus simply obtained from Eq. (12) with $\zeta = 0$ as

$$\left(\frac{\sigma_f}{\sigma_\theta}\right)^6 = F_0 + F_1\cos2\theta + F_2\cos4\theta + F_3\cos6\theta + F_4\cos8\theta + F_5\cos10\theta + F_6\cos12\theta, \tag{13}$$

and the yield stress under equal biaxial tension σ_b is obtained from Eq. (12) with $\zeta = 1$ and $\theta = 0$ as

$$\left(\frac{\sigma_f}{\sigma_b}\right)^6 = 2F_0 + 2G_0 + 2H_0 + N_0. \tag{14}$$

Axial yield stresses under pure shear stress at two loading orientation angles 0° and 45° are (the result for 90° is exactly the same as that for 0°)

$$\begin{aligned} \left(\frac{\sigma_f}{\sigma_{s0}}\right)^6 &= 2F_0 - 32F_4 + 64F_6 - 2G_0 - 4G_2 - 16G_4 + 2H_0 - N_0 - 2N_2, \\ \left(\frac{\sigma_f}{\sigma_{s45}}\right)^6 &= 2F_0 - 32F_4 - 64F_6 - 2G_0 + 4G_2 - 16G_4 + 2H_0 - N_0 + 2N_2. \end{aligned} \tag{15}$$

To emphasize the notion of intrinsic variables, we choose in this study $\sigma_{s\theta} = \sigma_1$ as the axial or normal yield stress under pure shear stress $\sigma_1 = -\sigma_2 > 0$ instead of τ_θ as used by Yoshida et al. [30]. Finally, biaxial tension yield stresses with a stress ratio of one half ($\zeta = 1/2$) at three loading orientation angles 0°, 45°, and 90° are given as

$$\begin{aligned} 64\left(\frac{\sigma_f}{\sigma_{p0}}\right)^6 =& 65F_0 + 63F_1 + 45F_2 + 27F_3 + 13F_4 + 3F_5 + F_6 + 34G_0 \\ &+ 30G_1 + 14G_2 + 6G_3 + 2G_4 + 20H_0 + 12H_1 + 8N_0 - 2N_2, \\ 64\left(\frac{\sigma_f}{\sigma_{p45}}\right)^6 =& 65F_0 - 45F_2 + 13F_4 - F_6 + 34G_0 - 14G_2 + 2G_4 + 20H_0 + 8N_0 + 2N_2, \\ 64\left(\frac{\sigma_f}{\sigma_{p90}}\right)^6 =& 65F_0 - 63F_1 + 45F_2 - 27F_3 + 13F_4 - 3F_5 + F_6 + 34G_0 \\ &- 30G_1 + 14G_2 - 6G_3 + 2G_4 + 20H_0 - 12H_1 + 8N_0 - 2N_2. \end{aligned} \tag{16}$$

Those yield stresses are referred to as near plane-strain tension yield stresses by Yoshida et al. [30].

3 Parameter identification of the sixth-order yield function

We are now ready to investigate in some greater details various types and numbers per type of measurements from simple mechanical tests that are needed to fully identify all material constants or equivalently all Fourier coefficients in a sixth-order yield function. In light of the results presented in Sect. 2 above, we prefer to use the sixteen independent Fourier coefficients (F_0, F_1, F_2, F_3, F_4, F_5, F_6, G_0, G_1, G_2, G_3, G_4, H_0, H_1, N_0, N_2) instead of the polynomial material constants ($A_1, \ldots, A_{16}$) as the basis for our investigation on the directional dependence of the yielding and plastic flow in an orthotropic sheet metal. On the other hand, we revert back to those polynomial material constants when better modeling of the multi-axial dependence of the yielding and plastic flow is of primary concern under either on-axis ($\theta = 0°$ or $\theta = 90°$) or off-axis ($0° < \theta < 90°$) loading conditions. If the 16 independent Fourier coefficients of ϕ_6 are determined, the corresponding 16 polynomial material constants of Φ_6 can be obtained straightforward via linear equations Eq. (31) in "Appendix A," and vice versa.

3.1 Types of mechanical tests needed for full parameter identification

When we have no any prior knowledge about the actual degree of planar anisotropy of a steel sheet, we need to collect at least sixteen experimental measurements from some simple mechanical tests for fully calibrating the sixth-order yield function. In principle, one may choose one among many possible sets of measurements to best characterize the directional and multi-axial dependence of the yielding and plastic flow of the steel sheet for a given application. Typically, as many measurements as possible from uniaxial tension tests may be included as they are easy to obtain and most widely available. But measurements from both uniaxial and biaxial tension tests are needed as it is already known that at least one measurement from biaxial tension is required for fully calibrating a fourth-order yield function [6].

The first question to ask is whether or not 14 uniaxial tension measurements such as seven pairs of (σ_θ, r_θ) and 2 equal biaxial tension measurements (σ_b, r_b) will be sufficient as a possible set of the required 16 experimental inputs. In other words, one needs to check if the sixteen equations from Eqs. (10), (11), (13), and (14) will be linearly independent or not. The short answer is no. For example, there are four Fourier coefficients in a planar isotropic sixth-order yield function per Eq. (18) (see details in Sect. 3.4) to be determined but one has only three independent measurements (σ_0, r_0, σ_b) from uniaxial and equal biaxial tension tests ($r_b = 1$ always holds per Eq. (11) for a planarly isotropic sheet).

For the more general case of the sixth-order yield function with maximum plastic anisotropy (i.e., with all sixteen independent Fourier coefficients being nonzero at the outset), there are up to seven independent uniaxial yield stress measurements σ_θ, that is, Eq. (13) contains only seven Fourier coefficients: (F_0, F_1, F_2, F_3, F_4, F_5, F_6). Similarly, there are possibly up to 12 independent uniaxial plastic strain ratio measurements r_θ: $F(\theta)$ and $G(\theta)$ in Eq. (10) contains only 12 out of a total of 16 independent Fourier constants, namely, (F_0, F_1, F_2, F_3, F_4, F_5, F_6, G_0, G_1, G_2, G_3, G_4). In fact, there are at most up to 12 possible independent measurements from all uniaxial tension tests because the seven Fourier coefficients in Eq. (13) are among the twelve ones in Eq. (10). Consequently, a total of up to 12 uniaxial tension measurements plus 2 equal biaxial tension measurements (σ_b, r_b) will not be sufficient to determine all sixteen Fourier coefficients. That is, at least two measurements from other biaxial tests such as pure shear stress or near plane-strain tension tests are then needed.

3.2 Full parameter identification using 12 uniaxial tension measurements

One can select various numbers of yield stresses and plastic strain ratios from uniaxial tension tests along at least six different loading orientation angles to constitute the 12 measurements needed for parameter identification. The only requirement is that those 12 uniaxial tension measurements are independent, that is, the twelve equations from Eqs. (10) and (13) are linearly independent. One obvious default choice is to first determine the seven Fourier coefficients (F_0, F_1, F_2, F_3, F_4, F_5, F_6) of $F(\theta)$ using seven uniaxial tension yield stresses per Eq. (13), say, such as (σ_0, σ_{15}, σ_{30}, σ_{45}, σ_{60}, σ_{75}, σ_{90}). Afterward, one can determine the other five coefficients (G_0, G_1, G_2, G_3, G_4) using five uniaxial plastic strain ratios per Eq. (10), for example, such as (r_0, $r_{22.5}$, r_{45}, $r_{67.5}$, r_{90}).

Once the twelve Fourier coefficients above have been determined from 12 independent uniaxial tension measurements, one can then determine $2H_0 + N_0$ using the equal biaxial tension yield stress σ_b per Eq. (14)

and subsequently H_1 using the equal biaxial tension plastic strain ratio r_b per Eq. (11) as long as $r_b \neq -1$. Similarly, one can use the two pure shear yield stresses σ_{s0} and σ_{s45} given in Eq. (15) to determine $2H_0 - N_0$ and N_2, respectively. The results of $2H_0 + N_0$ and $2H_0 - N_0$ determine H_0 and N_0 individually and thus complete the full parameter identification. Alternatively, one can use the first two near plane-strain tension yield stresses σ_{p0} and σ_{p45} in Eq. (16) to determine $5H_0 + 2N_0$ and N_2, respectively. The results of $2H_0 + N_0$ and $5H_0 + 2N_0$ also determine H_0 and N_0 individually.

One may select other combinations of biaxial test data to constitute the four measurements needed for determining those four Fourier coefficients (H_0, H_1, N_0, N_2) above. Again, the only requirement is that those four biaxial test measurements are independent so the four equations from Eqs. (11) and (12) with $\zeta = \sigma_2/\sigma_1 \neq 0$ are linearly independent. One can show that at least one of the biaxial tests should be carried out off-axis ($\theta \neq 0°$ and $\theta \neq 90°$). For example, four biaxial measurements (σ_b, r_b, σ_{p0}, σ_{p90}) or (σ_b, r_b, σ_{p0}, σ_{s0}) are not independent and will not be sufficient to determine all of those four Fourier coefficients. Detailed results of the default and other viable 12 uniaxial tension measurements for identifying the 12 Fourier coefficients (F_0, F_1, F_2, F_3, F_4, F_5, F_6, G_0, G_1, G_2, G_3, G_4) in Eqs. (10) and (13) are listed in "Appendix B" along with the separate results of using some viable biaxial test measurements described above for identifying the remaining four Fourier coefficients (H_0, H_1, N_0, N_2).

3.3 Full parameter identification using less uniaxial tension measurements

One may use additional yield stresses from other off-axis biaxial plane stress tests in the parameter identification so the yield function can better model the multi-axial plastic yielding of a steel sheet at a loading orientation angle θ. One question is then about the minimum number of measurements from off-axis tests that will be needed to fully account for the directional dependence of the yield function.[3] Per Eq. (4), on-axis test measurements ($\tau_{xy} = 0$) can only determine up to seven material constants $A_1, \ldots, A_7$. From Eqs. (10)–(14) by setting (if needed) $\theta = 0°$ and $\theta = 90°$ and using the results in "Appendix A," one can show that indeed the most common nine on-axis uniaxial and biaxial test measurements (σ_0, r_0, σ_{90}, r_{90}, σ_b, r_b, σ_{s0}, σ_{p0}, σ_{p90}) contain only those seven material constants. Besides the default choice of seven measurements (σ_0, r_0, σ_{90}, r_{90}, σ_b, r_b, σ_{p0} or σ_{s0}), other possibilities are (σ_0, r_0, σ_{90}, r_{90}, σ_b, σ_{p0}, σ_{p90}), (σ_0, r_0, σ_{90}, r_{90}, σ_b, σ_{p0}, σ_{s0}), and (σ_0, σ_{90}, σ_b, r_b, σ_{p0}, σ_{p90}, σ_{s0}). Details of using those and other measurements for determining the seven *on-axis* material constants $A_1, \ldots, A_7$ are given in "Appendix C."

So the remaining nine material constants $A_8, \ldots, A_{16}$ have to be determined from off-axis uniaxial and biaxial tests at a minimum of four or five different off-axis loading angles ($0° < \theta < 90°$). From Sect. 3.2 and related results given in "Appendix B," it is already known that up to eight measurements from off-axis uniaxial tension and at least one measurement from either off-axis pure shear σ_{s45} or off-axis near plane-strain tension σ_{p45} can be used as part of parameter identification of 16 Fourier coefficients. If the off-axis uniaxial tension measurements are limited to a pair of (σ_{45}, r_{45}) in single off-axis tension tests, then seven additional off-axis measurements can come from biaxial tests. Some examples of using more than one yield stress from off-axis pure shear and near plane-strain tension tests but less than eight yield stress and plastic strain ratio measurements from off-axis uniaxial tension tests for parameter identification of the nine *off-axis* material constants $A_8, \ldots, A_{16}$ are discussed in more details in "Appendix C" as well.

3.4 Parameter identification using limited experimental measurements

We now consider the situation most often encountered in practical industrial applications, that is, the actual total number of independent uniaxial and/or biaxial mechanical testing measurements available for a given steel sheet metal are less than the required 12 and 4, respectively. We first examine some sufficient conditions for dropping high-order sinusoids or cosine terms in $\phi_6(\sigma_1, \sigma_2, \theta)$ or equivalently for eliminating various types of earing formation in axi-symmetric deep drawing of a sheet metal [24], namely (recalling also results given in Eq. (9))

$$\text{(i) without any } \cos 12\theta \text{ terms:} \quad F_6 = 0,$$
$$\text{(ii) without any } \cos 10\theta \text{ terms:} \quad F_5 = 0,$$

[3] An on-axis loading is defined as when the axis of σ_1 or σ_2 coincides with the rolling and transverse directions of a sheet metal, that is, $\theta = 0°$ or $\theta = 90°$. So an off-axis loading is defined as $0° < \theta < 90°$. In terms of the Cartesian stress components, the on-axis and off-axis tests are specified with $\tau_{xy} = 0$ and $\tau_{xy} \neq 0$, respectively.

$$\begin{aligned}
&\text{(iii) without any } \cos 8\theta \text{ terms:} \quad F_4 = G_4 = 0,\\
&\text{(iv) without any } \cos 6\theta \text{ terms:} \quad F_3 = G_3 = 0,\\
&\text{(v) without any } \cos 4\theta \text{ terms:} \quad F_2 = G_2 = N_2 = 0,\\
&\text{(vi) without any } \cos 2\theta \text{ terms:} \quad F_1 = G_1 = H_1 = 0.
\end{aligned} \tag{17}$$

When all of these six constraints are imposed on the above 12 independent Fourier coefficients, it leads to a planar or in-plane isotropic yield function of six degrees with only four nonzero Fourier coefficients F_0, G_0, H_0, and N_0,

$$\phi_{6p}(\sigma_1, \sigma_2) = F_0(\sigma_1^6 + \sigma_2^6) + G_0(\sigma_1^5\sigma_2 + \sigma_1\sigma_2^5) + H_0(\sigma_1^4\sigma_2^2 + \sigma_1^2\sigma_2^4) + N_0\sigma_1^3\sigma_2^3. \tag{18}$$

Finally, a von Mises-like isotropic sixth-order yield function is simply the case of planar isotropy of a single experimental measurement of σ_0 with $r_\theta = r_b = 1$, $\sigma_b = \sigma_\theta = \sigma_0$, $\sigma_s = \sigma_0/\sqrt{3}$ (pure shear), namely (assuming $\sigma_f = \sigma_0$)

$$\phi_{6i}(\sigma_1, \sigma_2) = \sigma_1^6 - 3\sigma_1^5\sigma_2 + 6\sigma_1^4\sigma_2^2 - 7\sigma_1^3\sigma_2^3 + 6\sigma_1^2\sigma_2^4 - 3\sigma_1\sigma_2^5 + \sigma_2^6 = (\sigma_1^2 - \sigma_1\sigma_2 + \sigma_2^2)^3. \tag{19}$$

One may now seek to determine a sixth-order yield function of *reduced planar anisotropy* when a complete set of 16 independent experimental measurements such as those listed in "Appendix B" is not available for the steel sheet under consideration. At the minimum, we assume in the following that at least five measurements are always made available: (σ_0, r_0, σ_{90}, r_{90}) from two uniaxial tension tests and σ_b or r_b from an equal biaxial tension test.[4] Depending on any additional number of experimental measurements from off-axis uniaxial tension tests and other biaxial tests, one can systematically set some independent Fourier coefficients to be zero or other constant values first and then carry out the parameter identification on the rest of the reduced number of independent Fourier coefficients in the sixth-order yield function. Some of the common cases are discussed briefly in the following (for the equations to compute the relevant independent Fourier coefficients, see "Appendix D" for details):

(a) Ten uniaxial tension measurements Set both $F_5 = 0$ and $F_6 = 0$ so only ten nonzero Fourier coefficients are to be determined using measurements from five uniaxial tension tests with three of them being off-axis. A set of ten uniaxial tension measurements would be like (σ_0, σ_{θ_1}, σ_{45}, σ_{θ_2}, σ_{90}) and (r_0, r_{θ_1}, r_{45}, r_{θ_2}, r_{90}), where θ_1 is between 0° and 45°, and θ_2 is between 45° and 90°. One can determine the five Fourier coefficients (F_0, F_1, $F_2.F_3$, F_4) first using only the yield stresses and then the other five Fourier coefficients (G_0, G_1, G_2, G_3, G_4) using additional measurements of plastic strain ratios.

(b) Eight uniaxial tension measurements Set $F_4 = G_4 = F_5 = F_6 = 0$ so only eight nonzero Fourier coefficients are to be determined from four uniaxial tension tests with two of them being off-axis. A set of eight uniaxial tension measurements would be like (σ_0, σ_{45}, σ_{90}, σ_θ) and (r_0, r_{45}, r_{90}, r_θ), where θ is either between 0° and 45° or between 45° and 90°. One can determine the four Fourier coefficients (F_0, F_1, F_2, F_3) first using only the yield stresses and then the other four Fourier coefficients (G_0, G_1, G_2, G_3) with the addition of plastic strain ratios.

(c) Six uniaxial tension measurements Set $F_3 = G_3 = F_4 = G_4 = F_5 = F_6 = 0$ so only six nonzero Fourier coefficients (F_0, F_1, F_2, G_0, G_1, G_2) are to be determined using six measurements from three common uniaxial tension tests (two on-axis tests and only one off-axis test): (σ_0, r_0, σ_{45}, r_{45}, σ_{90}, r_{90}).

(d) Four uniaxial tension measurements Set $G_2 = F_2 = G_3 = F_3 = F_4 = G_4 = F_5 = F_6 = 0$ so only four nonzero Fourier coefficients (F_0, F_1, G_0, G_1) are to be determined from the two on-axis uniaxial tension tests: (σ_0, r_0, σ_{90}, r_{90}).

(e) Three on-axis and zero off-axis biaxial test measurements Set $N_2 = 0$ so only three remaining Fourier coefficients (H_0, H_1, N_0) are to be determined from on-axis biaxial tests. Two measurements from equal biaxial tension and one measurement from another on-axis biaxial test will be sufficient: such as (σ_b, r_b, σ_{p0}) or (σ_b, r_b, σ_{s0}).

[4] If only (σ_0, r_0) from a single uniaxial tension test are made available, one can simply set $\sigma_{90} = \sigma_0$, $\sigma_b = \sigma_0$ and $r_{90} = r_0$.

(f) Two on-axis and zero off-axis biaxial test measurements Set $H_1 = N_2 = 0$ so only two nonzero Fourier coefficients (H_0, N_0) are to be determined from two on-axis biaxial yield stresses such as (σ_b, σ_{p0}) or (σ_b, σ_{s0}). If two equal biaxial tension measurements (σ_b, r_b) are available, one can replace $H_1 = 0$ with $N_0 = -7$ per the von Mises isotropy to obtain H_0 and H_1.

(g) One on-axis and zero off-axis biaxial test measurement If only one measurement of either σ_b or r_b or any pure shear or near plane-strain tension yield stress such as those ones in Eqs. (15) or (16) is made available, one may set $H_1 = N_2 = 0$ and $N_0 = -7$ per the von Mises isotropy to obtain H_0. Alternatively (applicable to both cases (e) and (f) above, too), one may estimate some or all needed biaxial measurements r_b, σ_b, σ_{p0}, σ_{s0}, σ_{p45}, and σ_{s45} based on either Hill's 1948 quadratic yield function or Gotoh's 1977 fourth-order yield function and then determines the four Fourier coefficients (H_0, H_1, N_0, N_2) per Sect. 3.2.

4 Positivity and convexity testing of a calibrated yield function

Once all sixteen material constants in a homogeneous polynomial yield function of six degrees have been fully identified, its positivity and convexity should be certified next before applying it in any sheet metal forming analysis. It turns out that a convex homogeneous polynomial yield function of an even order is always positive for a nonzero stress (see a recent mathematical proof as Lemma 4.12 in [1]). So only the convexity of the polynomial yield function will need to be certified from now on. As part of the proposed calibration method and for completeness, we repeat the description about a numerical approach for convexity certification that was first given in [23], and it has since been successfully applied to many more calibrated Gotoh's fourth-order yield functions [26].

The sixth-order yield function $\Phi_6(\sigma_x, \sigma_y, \tau_{xy})$ of Eq. (4) is convex if and only if its Hessian matrix $\nabla^2\Phi_6$ is positive semi-definite for any applied plane stress on the yield surface $\Phi_6(\boldsymbol{\sigma}) - \sigma_f^6 = 0$. The sixth-order homogeneous polynomial yield function $\Phi_6(\sigma_x, \sigma_y, \tau_{xy})$ is twice differentiable, and its Hessian matrix is given as

$$\nabla^2\Phi_6(\sigma_x, \sigma_y, \tau_{xy}) = \begin{pmatrix} \frac{\partial^2\Phi_6}{\partial\sigma_x^2} & \frac{\partial^2\Phi_6}{\partial\sigma_x\partial\sigma_y} & \frac{\partial^2\Phi_6}{\partial\sigma_x\partial\tau_{xy}} \\ \frac{\partial^2\Phi_6}{\partial\sigma_y\partial\sigma_x} & \frac{\partial^2\Phi_6}{\partial\sigma_y^2} & \frac{\partial^2\Phi_6}{\partial\sigma_y\partial\tau_{xy}} \\ \frac{\partial^2\Phi_6}{\partial\tau_{xy}\partial\sigma_x} & \frac{\partial^2\Phi_6}{\partial\tau_{xy}\partial\sigma_y} & \frac{\partial^2\Phi_6}{\partial\tau_{xy}^2} \end{pmatrix}. \tag{20}$$

According to linear algebra (e.g., [4]), $\nabla^2\Phi_6$ is positive definite if all of its leading principal minors or subdeterminants (determinants of the k-by-k matrices in the upper left corner of $\nabla^2\Phi_6$, where $1 \le k \le 3$) are positive. If one defines

$$\Psi_{6A} = \frac{\partial^2\Phi_6}{\partial\sigma_x^2}, \quad \Psi_{6B} = \begin{vmatrix} \frac{\partial^2\Phi_6}{\partial\sigma_x^2} & \frac{\partial^2\Phi_6}{\partial\sigma_x\partial\sigma_y} \\ \frac{\partial^2\Phi_6}{\partial\sigma_y\partial\sigma_x} & \frac{\partial^2\Phi_6}{\partial\sigma_y^2} \end{vmatrix}, \quad \Psi_{6C} = |\nabla^2\Phi_6|, \tag{21}$$

then the strict convexity conditions of the sixth-order yield function are given as

$$\Psi_{6A}(\sigma_x, \sigma_y, \tau_{xy}) > 0, \quad \Psi_{6B}(\sigma_x, \sigma_y, \tau_{xy}) > 0, \quad \Psi_{6C}(\sigma_x, \sigma_y, \tau_{xy}) > 0. \tag{22}$$

By invoking the plane stress coordinate transformation relation Eq. (6), the above conditions may be rewritten in intrinsic variables instead as

$$\psi_{6A}(\sigma_1, \sigma_2, \theta) > 0, \quad \psi_{6B}(\sigma_1, \sigma_2, \theta) > 0, \quad \psi_{6C}(\sigma_1, \sigma_2, \theta) > 0. \tag{23}$$

Furthermore, by replacing the principal stresses (σ_1,σ_2) with their polar coordinate representation

$$\sigma_1 = \rho\cos\omega, \quad \sigma_2 = \rho\sin\omega, \quad \rho = \sqrt{\sigma_1^2 + \sigma_2^2} > 0, \quad 0^\circ \le \omega \le 180^\circ, \tag{24}$$

we finally reach a more practically usable form of convexity conditions for the yield function Φ_6 as (ρ is set to 1 without affecting the inequalities)

$$\psi_{6A}(\cos\omega, \sin\omega, \theta) > 0, \quad \psi_{6B}(\cos\omega, \sin\omega, \theta) > 0, \quad \psi_{6C}(\cos\omega, \sin\omega, \theta) > 0, \tag{25}$$

where $0° \le \omega \le 180°$ and $0° \le \theta \le 90°$. In an actual numerical evaluation of the above conditions of a fully calibrated sixth-order yield function, one will only need to find the minimum values of those three functions in ω and θ. The necessary and sufficient conditions for its strict convexity become

$$\min[\psi_{6A}(\cos\omega, \sin\omega, \theta)] > 0, \quad \min[\psi_{6B}(\cos\omega, \sin\omega, \theta)] > 0, \quad \min[\psi_{6C}(\cos\omega, \sin\omega, \theta)] > 0. \tag{26}$$

It is important to note that the above numerical certification of the convexity conditions takes very little computational time nowadays in practice and can be completed almost instantly on a laptop or desktop machine using *Matlab*, *Mathematica* or any similar numerical analysis tool.

5 A parameterized sixth-order yield function and its adjustments

If the sixth-order yield function Φ_6 or its equivalent ϕ_6 calibrated for a steel sheet turns out not to be strictly convex (i.e., it fails the convexity testing per Eq. (26)), there are at least two possible causes. One possibility is that the steel sheet under consideration is unusually highly textured and its anisotropic yielding and plastic flow behavior are beyond the applicability domain of a convex sixth-order yield function. If this is the case, one has to consider the use of even higher-order homogeneous polynomials as its convex yield function. The second possibility is that there may be some errors or uncertainties in the experimental input data that are used to calibrate the Fourier coefficients or polynomial material constants of the sixth-order yield function. If errors in the input data are deemed to be minor, one may make some slight adjustments on the input data or the identified Fourier coefficients so the convexity of the adjusted sixth-order yield function may be established.

By extending the approach first presented in [24], we propose here a parameterized version of the non-convex sixth-order yield function ϕ_6 with initially identified 16 independent Fourier coefficients and suggest an incremental adjustment procedure to find an approximate yield function $\phi_{6\xi}$ that is guaranteed to be convex. The parameterized yield function $\phi_{6\xi}$ has the same analytical form as ϕ_6 of Eq. (7), but its 16 independent Fourier coefficients $(f_0, \ldots, n_2)$ are defined in the following way:

$$\begin{aligned} &f_0 = 1 + (F_0 - 1)\xi_1, \quad f_1 = F_1\xi_2, \quad f_2 = F_2\xi_3, \quad f_3 = F_3\xi_4, \quad f_4 = F_4\xi_5, \quad f_5 = F_5\xi_6, \\ &f_6 = F_6\xi_7, \quad g_0 = -3 + (G_0 + 3)\xi_8, \; g_1 = G_1\xi_9, \quad g_2 = G_2\xi_{10}, \quad g_3 = G_3\xi_{11}, \quad g_4 = G_4\xi_{12}, \\ &h_0 = 6 + (H_0 - 6)\xi_{13}, \quad h_1 = H_1\xi_{14}, \quad n_0 = -7 + (N_0 + 7)\xi_{15}, \quad n_2 = N_2\xi_{16} \end{aligned} \tag{27}$$

where $\boldsymbol{\xi} = (\xi_1, \ldots, \xi_{16})$ are a set of 16 adjustable variables with initial values all being equal to 1. When the variables are set to their initial values $\xi_1 = \cdots = \xi_{16} = 1$, $\phi_{6\xi} = \phi_6$ of Eq. (7); when the variables are all set to zero, $\xi_1 = \cdots = \xi_{16} = 0$, $\phi_{6\xi} = \phi_{6i}$ of Eq. (19). As the isotropic sixth-order yield function is known to be convex for $\sigma_1^2 + \sigma_2^2 > 0$ (noting ϕ_{6i}=$(\sigma_1^2 - \sigma_1\sigma_2 + \sigma_2^2)^3$ and $\sigma_1^2 - \sigma_1\sigma_2 + \sigma_2^2$ is convex per Eq. (5) without A_4), one may always be able to find a suitable set of variables $\boldsymbol{\xi} = (\xi_1, \ldots, \xi_{16})$ with each of them being between 0 and 1 such that the parameterized sixth-order yield function $\phi_{6\xi}$ with its Fourier coefficients given by $(f_0, \ldots, n_2)$ of Eq. (27) can meet the convexity conditions of Eq. (26).

In practice, one can try at first to decrease one adjustable variable at a time from its initial value of 1 by a small increment such as 0.01 or 0.1 to see if such an adjustment can make the parameterized yield function $\phi_{6\xi}$ convex per Eq. (26). Otherwise, one can always set all adjustable variables to be the same, that is, $\xi_1 = \ldots = \xi_{16} = \xi$, and then decrease ξ gradually from its initial value of 1 by a small increment. The adjustment stops when $\phi_{6\xi}$ is found to be convex per Eq. (26) for the first time. A bisection search algorithm using larger increments initially and then smaller ones later may be part of an automatic adjustment process to achieve more precise results faster. If the variables $\boldsymbol{\xi} = (\xi_1, \ldots, \xi_{16})$ are all near to their initial values of 1, then $\phi_{6\xi}$ may be used as a good approximation of the initially as-calibrated Φ_6 of Eq. (4) or its equivalent ϕ_6 of Eq. (7) but now with the guaranteed convexity. On the other hand, if some or all adjustable variables are far less than 1, one may need to identify the specific bad input data used for parameter identification and repeat those experimental measurements as needed. Here, the potentially bad input data are those yield stress and/or plastic strain ratio measurements that deviate significantly from the ones predicted by the newly adjusted convex yield function $\phi_{6\xi}$.

In closing this Section, it is noted that the original polynomial yield function of six degrees Φ_6 with 16 material constants $A_1, \ldots, A_{16}$ can also be similarly parameterized as $\Phi_{6\xi}$ with its constants $a_1, \ldots, a_{16}$ being given as

Table 1 Various experimental measurement data for three steel sheet metals

Metal	DP780	DP980	LC Steel	Metal	DP780	DP980
Source	[30]	[30]	[28]	σ_{15}/σ_f	0.984	
σ_f/σ_0	1	1	1	$\sigma_{22.5}/\sigma_f$	0.963	1.001
σ_{45}/σ_f	0.963	1.011	1.0521	σ_{30}/σ_f	0.966	
σ_{90}/σ_f	1.030	1.023	0.9857	σ_{60}/σ_f	0.979	
r_0	0.51	0.73	2.04	$\sigma_{67.5}/\sigma_f$	0.989	1.012
r_{45}	1.27	0.91	1.27	σ_{75}/σ_f	1.016	
r_{90}	0.62	0.81	2.19	r_{15}	0.76	
σ_b/σ_f	1.019	1.010	1.1380	$r_{22.5}$	0.79	0.90
r_b			1.02	r_{30}	0.99	
σ_{p0}/σ_f			1.2556	r_{60}	1.16	
σ_{p45}/σ_f			1.2403	$r_{67.5}$	1.08	1.01
σ_{p90}/σ_f			1.2485	r_{75}	0.91	

$$\begin{aligned} &a_1 = 1 + (A_1 - 1)\xi_1, \quad a_2 = -3 + (A_2 + 3)\xi_2, \quad a_3 = 6 + (A_3 - 6)\xi_3, \quad a_4 = -7 + (A_4 + 7)\xi_4, \\ &a_5 = 6 + (A_5 - 6)\xi_5, \quad a_6 = -3 + (A_6 + 3)\xi_6, \quad a_7 = 1 + (A_7 - 1)\xi_7, \quad a_8 = 9 + (A_8 - 9)\xi_8, \\ &a_9 = -18 + (A_9 + 18)\xi_9, \quad a_{10} = 27 + (A_{10} - 27)\xi_{10}, \quad a_{11} = -18 + (A_{11} + 18)\xi_{11}, \\ &a_{12} = 9 + (A_{12} - 9)\xi_{12}, \quad a_{13} = 27 + (A_{13} - 27)\xi_{13}, \quad a_{14} = -27 + (A_{13} + 27)\xi_{14}, \\ &a_{15} = 27 + (A_{15} - 27)\xi_{15}, \quad a_{16} = 27 + (A_{16} - 27)\xi_{16} \end{aligned} \tag{28}$$

where the 16 adjustable variables $\boldsymbol{\xi} = (\xi_1, \ldots, \xi_{16})$ are again initially all being 1 for the as-calibrated yield function and all being 0 for the von Mises isotropic sheet. In general, they may not be of the same values as those used in Eq. (27). For example, $A_1 = 1$ if $\sigma_f = \sigma_0$ is assumed, then ξ_1 is not needed at all.

6 Applications to selected orthotropic steel sheets

To illustrate the actual working of the proposed calibration method, we applied it to three representative steel sheets in this Section: (i) a high strength dual-phase steel 780 HSS with 18 uniaxial tension measurements and one equal biaxial tension measurement; (ii) a high strength dual-phase steel 980 HSS with 10 uniaxial tension measurements and one equal biaxial tension measurement; and (iii) a low-carbon steel sheet with 6 uniaxial tension measurements and 5 biaxial tension measurements. The experimental measurement data of the first two steels were reported by Yoshida et al. [30], and the data for the third steel were given by Vegter et al. [28], respectively. Their measurement data are listed in Table 1 following the notations adapted in this study[5]. Following the common practice, $\sigma_f = \sigma_0$ was assumed, that is, the uniaxial tensile stress–strain curve along the rolling direction of each steel sheet was set to be the plastic work equivalent isotropic hardening stress–strain curve for the steel sheet.

Instead of using a reduced sixth-order yield function in terms of linearly transformed stresses with only 8 or 9 independent material constants to model these three steels as has been done by Aretz et al. [2] and Yoshida et al. [30], respectively, we considered here the complete sixth-order homogeneous polynomial yield function of Eq. (4) by incorporating the maximum of up to 16 independent experimental measurements allowable for each steel sheet. Based on the detailed analysis presented in Sect. 3 and the experimental data listed in Table 1, the sixth-order yield functions with 13, 11, and 10 independent material constants were used to model the 780 HSS, 980 HSS, and low-carbon steel sheets, respectively, in the following:

– *780 HSS*: a total number of the maximum allowable 12 independent uniaxial tension measurements (out of all 18 available measurements listed in Table 1) may be used to determine the 12 Fourier coefficients ($F_0, \ldots, F_6, G_0, \ldots, G_4$) per Sect. 3.2 and "Appendix B." In particular, we considered the two cases of (a) using seven yield stresses (σ_0, σ_{15}, σ_{30}, σ_{45}, σ_{60}, σ_{75}, σ_{90}) and five plastic strain ratios (r_0, $r_{22.5}$, r_{45}, $r_{67.5}$, r_{90}) and (b) using five yield stresses (σ_0, $\sigma_{22.5}$, σ_{45}, $\sigma_{67.5}$, σ_{90}) and seven plastic strain ratios (r_0, r_{15}, r_{30}, r_{45}, r_{60}, r_{75}, r_{90}) as the experimental inputs. As only one biaxial test measurement is available for this steel, the remaining four independent Fourier coefficients cannot be uniquely determined. By setting $H_1 = N_2 = 0$ and $N_0 = -7$ as suggested in Sect. 3.4(g), one can obtain the Fourier coefficient H_0 using the available equal biaxial tensile yield stress σ_b per Eq. (56.1).

[5] For simplicity, the three plane strain tension yield stresses reported for the low-carbon steel are regarded approximately as yield stresses under near plane-strain tension with $\sigma_1 = 2\sigma_2$.

Table 2 Fourier coefficient values of anisotropic functions $F(\theta)$, $G(\theta)$, $H(\theta)$ and $N(\theta)$ defined in Eq. (8)

Metal	DP780		DP980	LC Steel		von Mises
	Case (a)	Case (b)	Case (a)	Case (a)	Case (b)	
F_0	1.09164	1.12376	0.949412	0.891153	0.891153	1
F_1	0.0984529	0.106115	0.0541908	− 0.0451813	− 0.0451813	0
F_2	− 0.170982	− 0.146992	− 0.000118797	0.154028	0.154028	0
F_3	− 0.00453152	− 0.0158265	0.00957857	0	0	0
F_4	− 0.00534436	− 0.0374688	− 0.0130629	0	0	0
F_5	− 0.0126635	− 0.00903084	0	0	0	0
F_6	0.00343266	− 0.0205572	0	0	0	0
G_0	− 3.11697	− 3.24993	− 2.68651	− 3.36661	− 3.36661	− 3
G_1	− 0.0112231	− 0.109207	− 0.0538056	0.232510	0.232510	0
G_2	1.13766	0.99372	0.119907	− 0.892213	−0.892213	0
G_3	− 0.09112	0.0213943	− 0.0407748	0	0	0
G_4	0.0251055	0.158065	0.129390	0	0	0
H_0	5.97194	6.07277	5.70812	7.53992	7.63444	6
H_1	0	0	0	− 0.336313	− 0.336313	0
N_0	− 7	− 7	− 7	− 9.66860	− 9.85764	− 7
N_2	0	0	0	− 2.44412	−2.63315	0

- *980 HSS*: all available yield stresses (σ_0, $\sigma_{22.5}$, σ_{45}, $\sigma_{67.5}$, σ_{90}) and plastic strain ratios (r_0, $r_{22.5}$, r_{45}, $r_{67.5}$, r_{90}) from five uniaxial tension tests were used to determine the 10 Fourier coefficients ($F_0, \ldots, F_4$, $G_0, \ldots, G_4$) with $F_5 = F_6 = 0$ per Sect. 3.4(a) and "Appendices B and D". The situation for the remaining four independent Fourier coefficients is the same as above for 780 HSS. Again, by setting $H_1 = N_2 = 0$ and $N_0 = -7$ as suggested in Sect. 3.4(g), one can obtain the Fourier coefficient H_0 using the available equal biaxial tensile yield stress σ_b per Eq. (56.1).
- *Low-Carbon Steel*: very limited measurements from uniaxial tension are available for this low-carbon steel, so all three yield stresses ($\sigma_0, \sigma_{45}, \sigma_{90}$) and three plastic strain ratios (r_0, r_{45}, r_{90}) were used to determine the 6 Fourier coefficients (F_0, F_1, F_2, G_0, G_1, G_2) with $F_3 = G_3 = F_4 = G_4 = F_5 = F_6 = 0$ per Sect. 3.4(c) and "Appendix D." On the other hand, five experimental measurements ($\sigma_b, r_b, \sigma_{p0}, \sigma_{p45}, \sigma_{p90}$) from biaxial tension tests are available for this steel, see Table 1. The off-axis near plane-strain yield stress σ_{p45} has to be used, while only three out of the remaining four on-axis biaxial tension measurements are needed. In particular, we considered here the following two cases of (a) using ($\sigma_b, r_b, \sigma_{p0}, \sigma_{p45}$) and (b) using ($\sigma_b, r_b$, $\sigma_{p45}, \sigma_{p90}$) for determining the four Fourier coefficients (H_0, H_1, N_0, N_2) per Sect. 3.2 and "Appendix B."

Numerical values of 16 independent Fourier coefficients of five such sixth-order yield functions calibrated for the three steel sheets are summarized in Table 2, and the corresponding 16 polynomial material constants are given in Table 3 per Eq. (31) in "Appendix A." To be more precise for subsequent convexity testing, all Fourier coefficients and material constants are kept to six significant digits. Listed also in both tables are the values for the ideal von Mises isotropic material for comparison. As $\sigma_f = \sigma_0$ was used here (see Table 1) so $A_1 = 1$ in Table 3 for all sheet metals. On the other hand, the Fourier coefficients of each steel sheet with a value of either 0 or − 7 in Table 2 are those ones manually set in order to calibrate the rest of 16 independent Fourier coefficients due to lack of the required types and numbers per type of experimental measurements for each sheet metal.

The quality of the five calibrated sixth-order yield functions listed in Tables 2 and 3 may be better assessed by comparing their predictions with all available experimental measurements listed in Table 1 for these three steel sheets. As shown in Fig. 1a, the predicted directional dependence of normalized yield stresses σ_θ/σ_f and plastic strain ratios r_θ given by two calibrated sixth-order yield functions (a) and (b) for the dual-phase 780 HSS steel are compared with its 18 uniaxial tension experimental measurements. As only up to 12 uniaxial tension measurements were used in calibrating the two sixth-order yield functions (a) and (b), neither of them can fully capture the highly anisotropic yielding and plastic flow behavior of this steel under uniaxial tension. On the other hand, both yield functions give a very similar description for the yield/flow surfaces under on-axis biaxial tension ($\sigma_x \geq 0$, $\sigma_y \geq 0$ and $\tau_{xy} = 0$), the plastic flow direction in terms of the angle β under on-axis biaxial tension, and the yield/flow surfaces under one off-axis biaxial tension ($\sigma_1 \geq 0$, $\sigma_2 \geq 0$, and $\theta = 45°$), see Fig. 1b–d.[6] They match well with both available uniaxial and equal biaxial tension data as shown in either open or filled circles in those Figures.

[6] As shown in the insert of Figs. 1c, 2c or 3c, the angles α and β are computed from $\alpha = \tan^{-1}(\sigma_y/\sigma_x)$ and $\beta = \tan^{-1}(\dot{\varepsilon}^p_y/\dot{\varepsilon}^p_x)$, respectively. There is a symmetry in σ_1 and σ_2 of the yield/flow surfaces $\phi_6(\sigma_1, \sigma_2, \theta)$ for $\theta = 45°$ in Figs. 1d, 2d, and 3d.

Table 3 The material constant values of the sixth-order yield function $\Phi_6(\sigma_x, \sigma_y, \tau_{xy})$ defined in Eq. (4)

Metal	DP780		DP980	LC Steel		von Mises
	Case (a)	Case (b)	Case (a)	Case (a)	Case (b)	
A_1	1	1	1	1	1	1
A_2	− 2.02649	− 2.02649	− 2.53179	− 4.02632	− 4.02632	− 3
A_3	5.13695	4.58219	5.24115	9.16385	9.35289	6
A_4	− 7.00353	− 6.23997	− 6.43267	− 12.1127	− 12.4908	− 7
A_5	4.87191	4.66311	5.13552	9.83648	10.0255	6
A_6	− 1.92311	−1.92311	− 2.34263	−4.49134	− 4.49134	− 3
A_7	0.837484	0.837484	0.872461	1.09036	1.09036	1
A_8	9.83605	12.4057	8.66996	8.88445	8.88445	9
A_9	− 18.0526	−26.3732	− 18.5913	−24.044	− 24.4221	−18
A_{10}	21.3649	31.7834	30.3587	39.471	40.2272	27
A_{11}	− 18.4152	− 25.2477	− 18.9486	− 26.1386	− 26.5167	− 18
A_{12}	7.7219	10.2789	8.27716	9.71092	9.71092	9
A_{13}	32.341	29.8763	27.4097	25.4031	25.5921	27
A_{14}	− 22.8232	− 14.9584	− 30.5473	− 38.655	− 39.033	− 27
A_{15}	35.9184	29.7342	27.848	27.2768	27.4659	27
A_{16}	31.4614	31.8534	24.5155	24.8069	24.8069	27
$\xi_{\max}$	1.1	1.3	2.8	1.5	1.5	–

As there are no redundant experimental data and all 11 available measurements were used as inputs for parameter identification for the dual-phase 980 HSS steel, the predictions of the calibrated yield function match completely the experimental measurements, see Fig. 2a–d. Similar results are obtained for the low-carbon steel even though it has one redundant on-axis biaxial tension measurement. As shown in Fig. 3a–d, the yield function calibrated using either σ_{p0} or σ_{p90} gives identical results for uniaxial tension and very similar results for biaxial tension.

All five calibrated yield functions with its Fourier coefficients and polynomial material constants listed in Tables 2 and 3, respectively, were checked for strict convexity numerically per the necessary and sufficient conditions of Eq. (26). It turns out that all of them are verified to be strictly convex so no adjustments proposed in Sect. 5 are needed at all. They can thus be used with assurance of the desired mathematical attributes in a sheet metal forming analysis. To assess how far a particular sixth-order convex yield function as listed in Table 3 is from the convexity limit, we used the parameterized version of each calibrated yield function per Eq. (28) with $\xi_1 = \ldots = \xi_{16} = \xi$ and gradually *increase* the variable ξ from its initial value of 1 by an increment of 0.1 until the convexity conditions of Eq. (26) are violated. The maximum allowable ξ values to keep each yield function still convex are listed in Table 3. Using such a measure, the yield function calibrated for 980 HSS is farthest from the convexity limit with $\xi_{\max} = 2.8$, while the first calibrated yield function (a) of 780 HSS is closest to the convexity limit with $\xi_{\max} = 1.1$. It is interesting to note that the second yield function (b) for the same 780 HSS has a clearly higher maximum allowable $\xi_{\max} = 1.3$, indicating the effect of different uniaxial tension measurements on the convexity limit of the calibrated yield function. On the other hand, the two yield functions (a) and (b) calibrated for the low-carbon steel have the same maximum allowable $\xi_{\max} = 1.5$. The small increase in 0.1 in ξ from its initial value of 1 to reach the convexity limit for the parameterized yield function (a) of 780 HSS indicates that some caution may be warranted to keep any numerical runoff and other errors to a minimum level so the convexity of this particular yield/flow function used in an actual sheet metal forming analysis will not be violated.

7 Discussion and conclusions

In plane stress, a complete homogeneous sixth-order polynomial yield function admits up to 16 yield stresses and plastic strain ratios from both uniaxial and biaxial tension for calibrating its 16 material constants and thus has a much superior modeling capability of anisotropic yielding and flow behavior of a sheet metal in comparison with those of Hill's 1948 quadratic and Gotoh's 1977 fourth-order yield functions. The actual calibration of the sixth-order yield function still retains the same nice mathematical feature of those two earlier yield functions that requires a solution of a set of only *linear* equations.

By refining the approaches first used by Gotoh [6] and Hill [11,13], Gotoh's yield function was recast in terms of intrinsic variables and the parameter identification of its Fourier coefficients, and the necessary and sufficient conditions for positivity and convexity testing were recently examined in greater detail in [23–25].

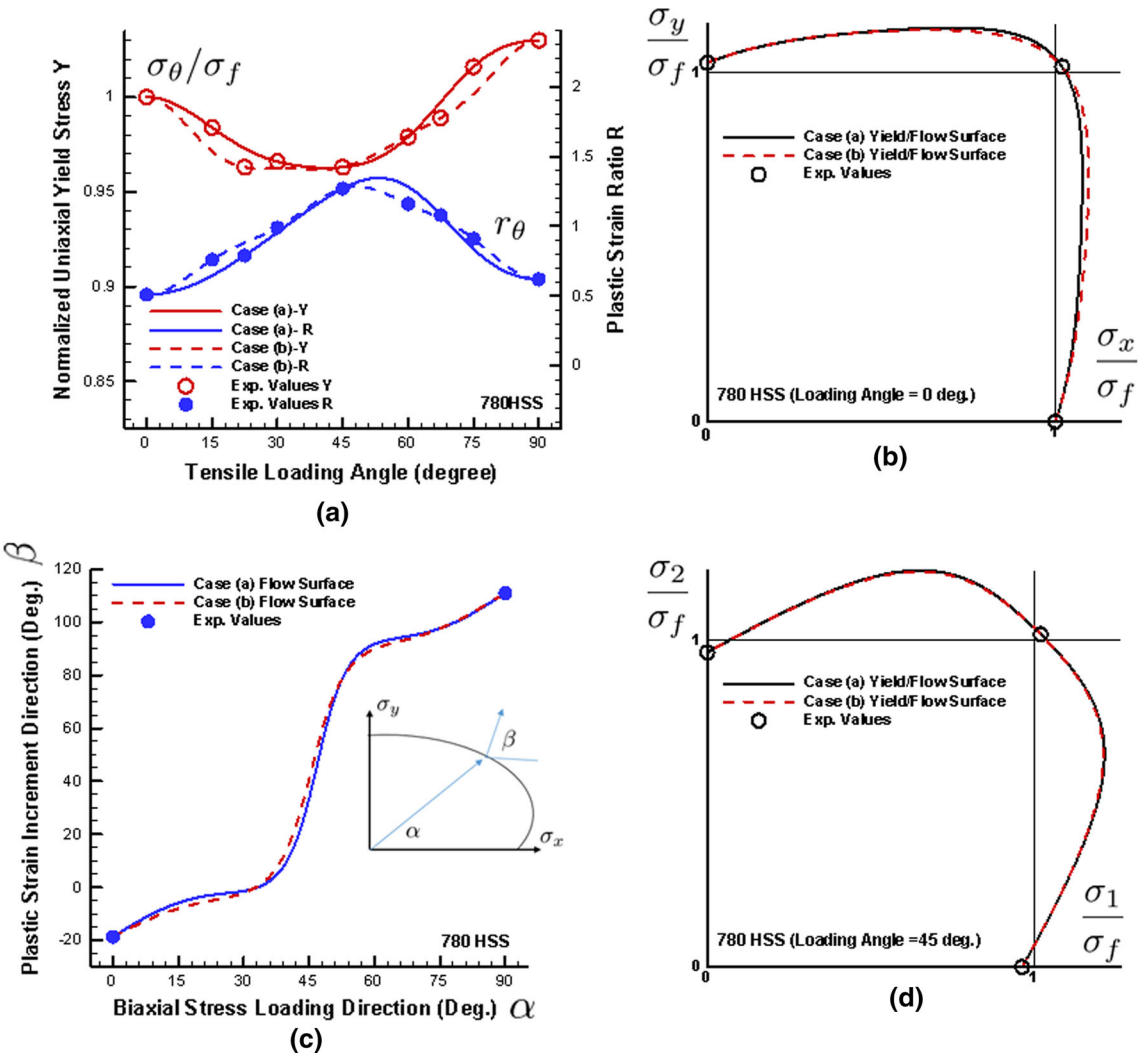

Fig. 1 Comparison between the predictions given by two calibrated sixth-order yield functions and experimental measurements for a DP780 steel sheet: **a** directional dependence of normalized yield stresses σ_θ/σ_0 and plastic strain ratios r_θ; **b** the yield/flow surfaces under on-axis biaxial tension ($\sigma_x \geq 0$, $\sigma_y \geq 0$ and $\tau_{xy} = 0$); **c** the plastic flow direction in terms of the angle β under on-axis biaxial tension; **d** the yield/flow surfaces under one off-axis biaxial tension ($\sigma_1 \geq 0$, $\sigma_2 \geq 0$, and $\theta = 45°$)

The same methodology has been shown in this study to be applicable to the sixth-order yield function as well. In particular, both the maximum number of uniaxial tension measurements and the minimum number of biaxial test measurements have now been identified to be 12 and 4, respectively, for fully calibrating the 16 material constants of the yield function. There is a greater flexibility in its parameter identification as one can choose one out of many sets of 16 independent uniaxial and biaxial test measurements depending on their availability and desired modeling capabilities. Furthermore, when the available experimental measurements are rather limited for a given sheet metal, a systematic approach can be used to eliminate some higher-order sinusoids (i.e., by setting some Fourier coefficients to be the values of an isotropic solid) in the recast yield function, and the remaining independent Fourier coefficients anywhere between 1 and 16 can still be identified.

A complete homogeneous sixth-order polynomial yield function would perform either the same or superior in comparison with the sixth-order yield functions formulated in terms of linearly transformed stresses, see [3] and [21]. In fact, those yield functions are of reduced sixth-order yield functions with less than 16 independent material constants but have one advantage being positive and convex a priori (if its nonlinear parameter identification procedure produces all real-valued constants). The direct method presented here divides up the parameter identification and convexity testing into two separate and sequential stages instead. Nevertheless, once a sixth-order yield function is fully calibrated, its strict convexity can be numerically verified per the

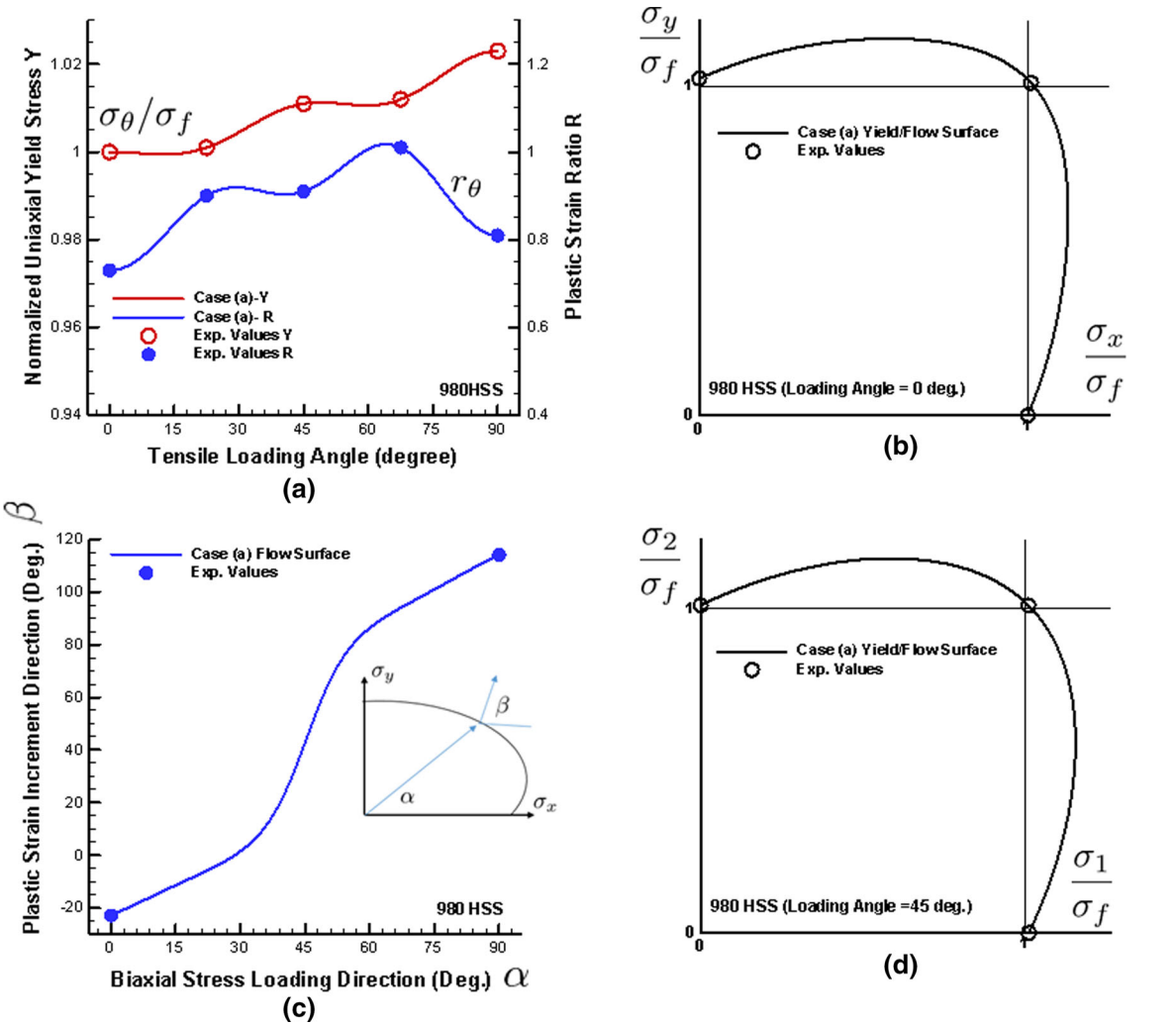

Fig. 2 Comparison between the predictions given by one calibrated sixth-order yield function and experimental measurements for a DP980 steel sheet: **a** directional dependence of normalized yield stresses σ_θ/σ_0 and plastic strain ratios r_θ; **b** the yield/flow surface under on-axis biaxial tension ($\sigma_x \geq 0$, $\sigma_y \geq 0$ and $\tau_{xy} = 0$); **c** the plastic flow direction in terms of the angle β under on-axis biaxial tension; **d** the yield/flow surface under one off-axis biaxial tension ($\sigma_1 \geq 0$, $\sigma_2 \geq 0$, and $\theta = 45°$).

necessary and sufficient conditions of Eq. (26). If needed, one can bring any calibrated but non-convex yield function back into the convex hull by an incremental adjustment approach described in Sect. 5. The yielding and plastic flow of 780 HSS steel under uniaxial tension exhibit unusually strong anisotropy (directional dependence) as neither of two calibrated yield functions can fully describe the observed behavior in terms of 18 uniaxial tension measurements (i.e., at least any two out of a total of 9 uniaxial tensile yield stresses and a total of four uniaxial tension measurements are redundant). One can definitely be able to use the standard least-square optimization to obtain the 12 Fourier coefficients (F_0,…,G_4) that best describe the overall uniaxial tension measurements. If these measurements are of very high quality and one wants to be able to incorporate all of them for anisotropic plasticity modeling of this steel sheet, then an even higher-order homogeneous polynomial yield function such as eighth-order one may have to be used.

As a cursory exercise, we applied also the convexity testing per Eq. (26) to the three calibrated sixth-order yield functions obtained by Soare et al. [22]. Using the 16 polynomial material constants listed in their Table 3, our numerical evaluation results showed that two of their yield functions (for Mat_1 and Mat_2 in their paper) are found to be strictly convex but their sixth-order yield function as calibrated for AA2090-T3 aluminum sheet failed the convexity test. In fact, their sixth-order yield function for AA2090-T3 was found to be strictly positive (as the minimum value of ϕ_6 is positive) but not convex (all minimum values of leading principal minors ψ_{6A}, ψ_{6B}, and ψ_{6C} are negative). Again, a nonlinear optimization method with many convexity constraints was

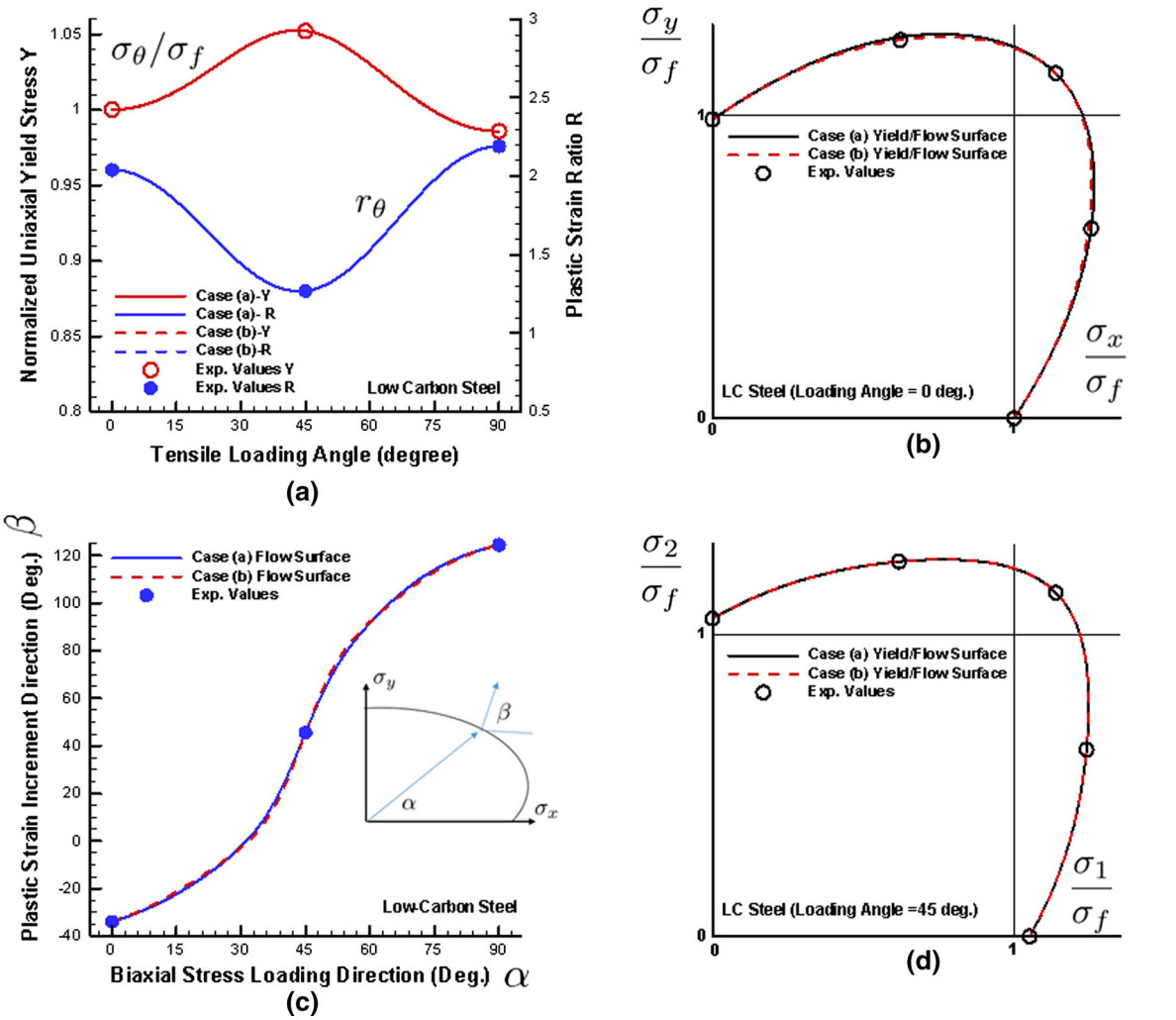

Fig. 3 Comparison between the predictions given by two calibrated sixth-order yield functions and experimental measurements for a low-carbon steel sheet: **a** directional dependence of normalized yield stresses σ_θ/σ_0 and plastic strain ratios r_θ; **b** the yield/flow surfaces under on-axis biaxial tension ($\sigma_x \geq 0$, $\sigma_y \geq 0$ and $\tau_{xy} = 0$); **c** the plastic flow direction in terms of the angle β under on-axis biaxial tension; **d** the yield/flow surfaces under one off-axis biaxial tension ($\sigma_1 \geq 0$, $\sigma_2 \geq 0$, and $\theta = 45°$)

used in [22] to obtain the set of 16 polynomial material constants for AA2090-T3 sheet. Although according to Soare et al. [22] that "it is sufficient to enforce these inequalities only along a discrete set of meridians and parallels of the unit sphere. Although we do not have a general proof for this assertion, this was always the case for fourth, sixth and eighth-order polynomials.", it is shown here that the specific convexity constraints imposed in their calibration method are actually only necessary but not sufficient at all. If we use again the parameterized version of their yield function per Eq. (28) with $\xi_1 = \cdots = \xi_{16} = \xi$ and gradually *decrease* the variable ξ from its initial value of 1 by an increment of 0.01, we found that we can make the parameterized version of their sixth-order yield function strictly convex by keeping $\xi \leq 0.96$. Such a small adjustment on their material constants indicated that the non-convexity of their yield function for AA2090-T3 might also be largely due to some numerical runoff errors in their optimized results.

Even though isotropic hardening was assumed at the outset in this study for the sixth-order polynomial yield function. That is, the 16 polynomial coefficients $(A_1, \ldots, A_{16})$ are regarded to be constant and may thus need to be calibrated only once. If all experimental inputs are however expressed as continuous functions of the accumulated equivalent plastic strain $\bar{\varepsilon}^p$ or plastic work per unit volume $\bar{W}^p$, the same linear equations given in "Appendices A–D" can also be used to obtain explicit algebraic expressions of these 16 material parameters as continuous functions of either $\bar{\varepsilon}^p$ or $\bar{W}^p$. The calibrated yield function $\Phi_6(\boldsymbol{\sigma}, \bar{\varepsilon}^p)$ or $\Phi_6(\boldsymbol{\sigma}, \bar{W}^p)$ will then be able to model the anisotropic strain or work hardening behavior of sheet metals without much difficulties at all.

One may also use experimental inputs at selected equivalent plastic strain or plastic work levels to calibrate the corresponding material parameters and adopt a multi-linear interpolation scheme similar to the one described by Yoshida et al. [31] to represent the continuous dependence of polynomial material parameters on the plastic strain or work hardening variable. By adding $\bar{\varepsilon}^p$ or $\bar{W}^p$ as the third variable in the convexity conditions Eq. (26) in addition to ω and θ, one can also numerically certify the convexity (makes necessary adjustments if needed) of an anisotropic hardening sixth-order polynomial yield function over the entire plastic deformation history up to the necking or fracture with a relatively small additional computational cost.

The plane stress sixth-order polynomial yield function $\Phi_6(\sigma_x, \sigma_y, \tau_{xy})$ may also be extended to 3D stress states for practical sheet metal forming analyses. If the contact friction between the tooling and a thin sheet metal is negligible, there will only be an additional normal stress σ_z but no out-of-plane shear stresses τ_{yz} and τ_{zx} acting on the sheet metal surfaces. The same 2D yield function $\Phi_6(\sigma_x, \sigma_y, \tau_{xy})$ can be used but in the form of $\Phi_6(\sigma_x - \sigma_z, \sigma_y - \sigma_z, \tau_{xy})$ in this reduced 3D stress state. For a general 3D stress state, a yield function in the form of $\Phi_6^{3D}(\sigma_x - \sigma_z, \sigma_y - \sigma_z, \tau_{xy}, \tau_{yz}, \tau_{zx})$ has to be used. However, a complete 3D sixth-order homogeneous polynomial yield function in terms of these five stress variables will have a total of 60 material constants (44 of them are related to the nonzero out-of-plane shear stresses) [20,32]. As those 44 extra material constants are too numerous to be practically calibrated using experimental inputs, two reduced versions of the 3D yield function are suggested instead [26],

$$\begin{aligned}
\Phi_{6a}^{3D}(\boldsymbol{\sigma}) &= \Phi_6(\sigma_x - \sigma_z, \sigma_y - \sigma_z, \pm\sqrt{\tau_{xy}^2 + \tau_{yz}^2 + \tau_{zx}^2}) + (A_{17} - A_{16})\tau_{yz}^6 + (A_{18} - A_{16})\tau_{zx}^6, \\
\Phi_{6b}^{3D}(\boldsymbol{\sigma}) &= \Phi_6(\sigma_x - \sigma_z, \sigma_y - \sigma_z, \tau_{xy}) + A_{17}\tau_{yz}^6 + A_{18}\tau_{zx}^6.
\end{aligned} \tag{29}$$

That is, τ_{xy}^2 in $\Phi_6(\sigma_x, \sigma_y, \tau_{xy})$ is replaced with $\tau_{xy}^2 + \tau_{yz}^2 + \tau_{zx}^2$ to partly account for the out-of-plane shear stresses in Φ_{6a}^{3D}. Two additional material constants A_{17} and A_{18} are added if two additional yield stresses from out-of-plane pure shear stress tests are available (otherwise setting $A_{17} = A_{18} = A_{16}$ for both Φ_{6a}^{3D} and Φ_{6b}^{3D}). The reduced 3D yield function Φ_{6a}^{3D} with $A_{17} = A_{18} = A_{16}$ is similar in form to the reduced fourth-order 3D yield function suggested by Hu [17], and the reduced 3D yield function Φ_{6b}^{3D} with $A_{17} = A_{18} = A_{16}$ is identical to the one proposed by Yoshida et al. [30]. The proposed two reduced 3D yield functions remain convex if the 2D yield function $\Phi_6(\sigma_x, \sigma_y, \tau_{xy})$ is convex and the two additional material constants A_{17} and A_{18} are larger than A_{16} in Φ_{6a}^{3D} or positive in Φ_{6b}^{3D}.

In summary, a direct and versatile calibration method has been proposed to first identify all of 16 independent Fourier coefficients of a complete sixth-order homogeneous polynomial yield function using anywhere between 1 and 16 available independent uniaxial and biaxial test measurements. Various linear equations and some analytical results from the solutions of those linear equations are presented in "Appendices A–D" for computing either the 16 Fourier coefficients or the 16 polynomial material constants using various types and numbers per type of independent experimental inputs. The calibrated yield function can then be checked for its convexity by numerically solving a set of relatively simple minimization problems. If the calibrated yield function is found to be concave, an incremental adjustment approach using a parameterized version of the as-calibrated yield function may then be used to obtain an approximate but convex yield function for a given steel sheet metal. Such a calibrated complete sixth-order homogeneous polynomial yield function with guaranteed convexity may then be extended to 3D stress states and used with confidence to obtain a stable and unique solution in a finite element analysis of sheet metal plastic forming processes.

Appendix A: Relations between Fourier coefficients and polynomial material constants

Results are listed for the 25 nonzero Fourier coefficients of four in-plane anisotropic functions $F(\theta)$, $G(\theta)$, $H(\theta)$, and $N(\theta)$ in Eq. (8) of $\phi_6(\sigma_1, \sigma_2, \theta)$ per Eq. (7) in terms of the 16 polynomial material constants $\boldsymbol{A} = (A_1, \ldots, A_{16})^T$ of the sixth-order yield function $\Phi_6(\sigma_x, \sigma_y, \tau_{xy})$ per Eq. (4):

$$\begin{aligned}
1024F_0 &= (231, 21, 7, 5, 7, 21, 231, 21, 7, 5, 7, 21, 7, 5, 7, 5)\boldsymbol{A}, \\
256F_1 &= (99, 6, 1, 0, -1, -6, -99, 6, 1, 0, -1, -6, 1, 0, -1, 0)\boldsymbol{A}, \\
2048F_2 &= (495, -15, -17, -15, -17, -15, 495, -15, -17, -15, -17, -15, -17, -15, -17, -15)\boldsymbol{A}, \\
512F_3 &= (55, -10, -3, 0, 3, 10, -55, -10, -3, 0, 3, 10, -3, 0, 3, 0)\boldsymbol{A},
\end{aligned}$$

$$
\begin{aligned}
1024F_4 &= (33,-13,1,3,1,-13,33,-13,1,3,1,-13,1,3,1,3)\boldsymbol{A},\\
512F_5 &= (3,-2,1,0,-1,2,-3,-2,1,0,-1,2,1,0,-1,0)\boldsymbol{A},\\
2048F_6 &= (1,-1,1,-1,1,-1,1,-1,1,-1,1,-1,1,-1,1,-1)\boldsymbol{A},\\
512G_0 &= (63,133,31,21,31,133,63,-7,11,9,11,-7,-9,-3,-9,-15)\boldsymbol{A},\\
64G_1 &= (9,26,3,0,-3,-26,-9,-2,1,0,-1,2,-1,0,1,0)\boldsymbol{A},\\
1024G_2 &= (-45,205,-45,-51,-45,205,-45,-19,-13,-19,-13,-19,19,13,19,45)\boldsymbol{A},\\
128G_3 &= (-15,10,-5,0,5,-10,15,2,-1,0,1,-2,3,0,-3,0)\boldsymbol{A},\\
512G_4 &= (-39,19,-7,3,-7,19,-39,15,-3,-1,-3,15,1,-5,1,-9)\boldsymbol{A},\\
128G_5 &= (-3,2,-1,0,1,-2,3,2,-1,0,1,-2,-1,0,1,0)\boldsymbol{A},\\
1024G_6 &= -3(1,-1,1,-1,1,-1,1,-1,1,-1,1,-1,1,-1,1,-1)\boldsymbol{A},\\
1024H_0 &= (105,155,329,171,329,155,105,-5,-23,11,-23,-5,9,-21,9,75)\boldsymbol{A},\\
256H_1 &= (15,30,101,0,-101,-30,-15,-2,-11,0,11,2,5,0,-5,0)\boldsymbol{A},\\
2048H_2 &= (-255,-225,257,-225,257,-225,-255,31,1,31,1,31,1,31,1,-225)\boldsymbol{A},\\
512H_3 &= (-45,-50,49,0,-49,50,45,14,17,0,-17,-14,-15,0,15,0)\boldsymbol{A},\\
1024H_4 &= (15,-35,47,-51,47,-35,15,-3,15,-19,15,-3,-17,13,-17,45)\boldsymbol{A},\\
512H_5 &= 5(3,-2,1,0,-1,2,-3,-2,1,0,-1,2,1,0,-1,0)\boldsymbol{A},\\
2048H_6 &= 15(1,-1,1,-1,1,-1,1,-1,1,-1,1,-1,1,-1,1,-1)\boldsymbol{A},\\
256N_0 &= (25,35,57,147,57,35,25,-1,-3,-17,-3,-1,1,11,1,-25)\boldsymbol{A},\\
512N_2 &= (-75,-85,-75,171,-75,-85,-75,11,21,11,21,11,-11,-21,-11,75)\boldsymbol{A},\\
256N_4 &= (15,5,-17,21,-17,5,15,-7,-5,9,-5,-7,7,-3,7,-15)\boldsymbol{A},\\
512N_6 &= -5(1,-1,1,-1,1,-1,1,-1,1,-1,1,-1,1,-1,1,-1)\boldsymbol{A}.
\end{aligned}
\tag{30}
$$

Among the 25 Fourier coefficients above, only 16 of them are linearly independent. One such set of 16 independent Fourier coefficients is $\boldsymbol{F}$=(F_0, F_1, F_2, F_3, F_4, F_5, F_6, G_0, G_1, G_2, G_3, G_4, H_0, H_1, N_0, N_2)^T. The remaining nine Fourier coefficients are linearly related to those Fourier coefficients as given in Eq. (9). The polynomial material constants $\boldsymbol{A} = (A_1, \ldots, A_{16})^T$ are uniquely and linearly related to those 16 Fourier coefficients as well from $\boldsymbol{A} = \boldsymbol{CF}$ where the 16-by-16 non-singular matrix $\boldsymbol{C}$ is given as

$$
\begin{pmatrix}
1 & 1 & 1 & 1 & 1 & 1 & 1 & 0 & 0 & 0 & 0 & 0 & 0 & 0 & 0 & 0\\
0 & 0 & 0 & 0 & 0 & -4 & -6 & 1 & 1 & 1 & 1 & 1 & 0 & 0 & 0 & 0\\
0 & 0 & -1 & -3 & -9 & 5 & 15 & 0 & 0 & -1 & -2 & -4 & 1 & 1 & 0 & -\frac{1}{2}\\
0 & 0 & 0 & 0 & 16 & 0 & -20 & 0 & 0 & 0 & 0 & 6 & 0 & 0 & 1 & 1\\
0 & 0 & -1 & 3 & -9 & -5 & 15 & 0 & 0 & -1 & 2 & -4 & 1 & -1 & 0 & -\frac{1}{2}\\
0 & 0 & 0 & 0 & 0 & 4 & -6 & 1 & -1 & 1 & -1 & 1 & 0 & 0 & 0 & 0\\
1 & -1 & 1 & -1 & 1 & -1 & 1 & 0 & 0 & 0 & 0 & 0 & 0 & 0 & 0 & 0\\
6 & 4 & -2 & -12 & -26 & -40 & -60 & -1 & -1 & -1 & -1 & -1 & 0 & 0 & 0 & 0\\
6 & 2 & -8 & -24 & -40 & 80 & 240 & 4 & 2 & -2 & -10 & -20 & -2 & -2 & 0 & 1\\
6 & 0 & -12 & 0 & 132 & 0 & -360 & 4 & 0 & -6 & 0 & 42 & 2 & 0 & -3 & 0\\
6 & -2 & -8 & 24 & -40 & -80 & 240 & 4 & -2 & -2 & 10 & -20 & -2 & 2 & 0 & 1\\
6 & -4 & -2 & 12 & -26 & 40 & -60 & -1 & 1 & -1 & 1 & -1 & 0 & 0 & 0 & 0\\
9 & 3 & -8 & 0 & 64 & 80 & 240 & -4 & -2 & 3 & 12 & 24 & 1 & 1 & 0 & -\frac{1}{2}\\
12 & 0 & -16 & 0 & -32 & 0 & -480 & -2 & 0 & 2 & 0 & -32 & -4 & 0 & 3 & -3\\
9 & -3 & -8 & 0 & 64 & -80 & 240 & -4 & 2 & 3 & -12 & 24 & 1 & -1 & 0 & -\frac{1}{2}\\
2 & 0 & 0 & 0 & -32 & 0 & -64 & -2 & 0 & 4 & 0 & -16 & 2 & 0 & -1 & 2
\end{pmatrix}.
\tag{31}
$$

Appendix B: List of equations for Fourier coefficients using twelve uniaxial tensile measurements

Some examples of linear equations for computing the first 12 (F_0, F_1, F_2, F_3, F_4, F_5, F_6, G_0, G_1, G_2, G_3, G_4) of the 16 independent Fourier coefficients given in "Appendix A" are listed here using 12 uniaxial ten-

sion measurements. First, one obtains the following first seven (F_0, F_1, F_2, F_3, F_4, F_5, F_6) of the 12 Fourier coefficients using a set of seven uniaxial tensile yield stresses (σ_0, σ_{15}, σ_{30}, σ_{45}, σ_{60}, σ_{75}, σ_{90}),

$$\begin{pmatrix} F_0 \\ F_1 \\ F_2 \\ F_3 \\ F_4 \\ F_5 \\ F_6 \end{pmatrix} = \frac{1}{6} \begin{pmatrix} \frac{1}{2} & 1 & 1 & 1 & 1 & 1 & \frac{1}{2} \\ 1 & \sqrt{3} & 1 & 0 & -1 & -\sqrt{3} & -1 \\ 1 & 1 & -1 & -2 & -1 & 1 & 1 \\ 1 & 0 & -2 & 0 & 2 & 0 & -1 \\ 1 & -1 & -1 & 2 & -1 & -1 & 1 \\ 1 & -\sqrt{3} & 1 & 0 & -1 & \sqrt{3} & -1 \\ \frac{1}{2} & -1 & 1 & -1 & 1 & -1 & \frac{1}{2} \end{pmatrix} \begin{pmatrix} \tilde{\sigma}_0^6 \\ \tilde{\sigma}_{15}^6 \\ \tilde{\sigma}_{30}^6 \\ \tilde{\sigma}_{45}^6 \\ \tilde{\sigma}_{60}^6 \\ \tilde{\sigma}_{75}^6 \\ \tilde{\sigma}_{90}^6 \end{pmatrix}, \tag{32}$$

where $\tilde{\sigma}_\theta = \sigma_f / \sigma_\theta$[7].

Next, one can obtain the other five Fourier coefficients (G_0, G_1, G_2, G_3, G_4) by adding the five uniaxial plastic strain ratios (r_0, $r_{22.5}$, r_{45}, $r_{67.5}$, r_{90}) and by solving a set of five linear equations. The results are

$$\begin{pmatrix} G_0 \\ G_1 \\ G_2 \\ G_3 \\ G_4 \end{pmatrix} = \frac{1}{24} \begin{pmatrix} 3 & 6 & 6 & 6 & 3 \\ 6 & 6\sqrt{2} & 0 & -6\sqrt{2} & -6 \\ 6 & 0 & -12 & 0 & 6 \\ 6 & -6\sqrt{2} & 0 & 6\sqrt{2} & -6 \\ 3 & -6 & 6 & -6 & 3 \end{pmatrix} \begin{pmatrix} T_1 \\ T_2 \\ T_3 \\ T_4 \\ T_5 \end{pmatrix} \tag{33}$$

where

$$\begin{pmatrix} T_1 \\ T_2 \\ T_3 \\ T_4 \\ T_5 \end{pmatrix} = \begin{pmatrix} -\frac{6r_0(F_0+F_1+F_2+F_3+F_4)+2(r_0-2)F_5-6F_6}{1+r_0} \\ \frac{3r_{22.5}(-2F_0-\sqrt{2}F_1+\sqrt{2}F_3+2F_4)+\sqrt{2}(r_{22.5}-2)F_5}{1+r_{22.5}} \\ -\frac{6r_{45}(F_0-F_2+F_4)+6F_6}{1+r_{45}} \\ \frac{3r_{67.5}(-2F_0+\sqrt{2}F_1-\sqrt{2}F_3+2F_4)-\sqrt{2}(r_{67.5}-2)F_5}{1+r_{67.5}} \\ \frac{-6r_{90}(F_0-F_1+F_2-F_3+F_4)+2(r_{90}-2)F_5+6F_6}{1+r_{90}} \end{pmatrix}. \tag{34}$$

An alternative choice of a set of five uniaxial plastic strain ratios is (r_0, r_{30}, r_{45}, r_{60}, r_{90}), and the first five Fourier coefficients in $G(\theta)$ are given as

$$\begin{pmatrix} G_0 \\ G_1 \\ G_2 \\ G_3 \\ G_4 \end{pmatrix} = \frac{1}{12} \begin{pmatrix} 2 & 2 & 0 & 2 & 2 \\ 4 & 2 & 0 & -2 & -4 \\ 3 & 0 & -6 & 0 & 3 \\ 2 & -2 & 0 & 2 & -2 \\ 1 & -2 & 6 & -2 & 1 \end{pmatrix} \begin{pmatrix} T_1 \\ T_2 \\ T_3 \\ T_4 \\ T_5 \end{pmatrix} \tag{35}$$

where

$$\begin{pmatrix} T_1 \\ T_2 \\ T_3 \\ T_4 \\ T_5 \end{pmatrix} = \begin{pmatrix} -\frac{6r_0(F_0+F_1+F_2+F_3+F_4)+2(r_0-2)F_5-6F_6}{1+r_0} \\ \frac{6r_{30}(-2F_0-F_1+F_2+2F_3+F_4)-2(r_{30}-2)F_5+12F_6}{1+r_{30}} \\ -\frac{6r_{45}(F_0-F_2+F_4)+6F_6}{1+r_{45}} \\ \frac{6r_{60}(-2F_0+F_1+F_2-2F_3+F_4)+2(r_{60}-2)F_5+12F_6}{1+r_{60}} \\ \frac{-6r_{90}(F_0-F_1+F_2-F_3+F_4)+2(r_{90}-2)F_5+6F_6}{1+r_{90}} \end{pmatrix}. \tag{36}$$

[7] It is noted that this yield stress ratio is the inverse of the conventional normalized yield stress as shown in Table 1. We will use the new yield stress ratios in all Appendices in this study.

To better describe the directional dependence of plastic flow, one can use seven plastic strain ratios (r_0, r_{15}, r_{30}, r_{45}, r_{60}, r_{75}, r_{90}) and five yield stresses (σ_0, $\sigma_{22.5}$, σ_{45}, $\sigma_{67.5}$, σ_{90}) or (σ_0, σ_{30}, σ_{45}, σ_{60}, σ_{90}) from uniaxial tension tests for determining the above twelve Fourier coefficients. One can also use various six yield stresses and six plastic strain ratios from uniaxial tension tests, such as (σ_0, σ_{30}, σ_{45}, σ_{60}, σ_{75}, σ_{90}) and (r_0, r_{15}, r_{30}, r_{45}, r_{60}, r_{90}). If uniaxial tension tests of a steel sheet have been conducted at only six different loading orientation angles, then all of these six pairs of yield stresses and plastic strain ratios may be used to form a set of twelve linearly independent equations and to obtain the 12 Fourier coefficients (F_0, F_1, F_2, F_3, F_4, F_5, F_6, G_0, G_1, G_2, G_3, G_4) by solving these twelve linear equations together. All cases mentioned above are viable choices as the 12-by-12 matrix of their linear equations for each case is found to be non-singular.

Thirdly, two measurements from an equal biaxial tension test are used to help determining the remaining four Fourier coefficients (H_0, H_1, N_0, N_2). The equal biaxial tension yield stress σ_b is used to determine $2H_0 + N_0$, and the equal biaxial plastic strain ratio $r_b \neq -1$ is then used to determine H_1. Two additional measurements from other biaxial tests are used to complete the determination of these four Fourier coefficients. If the two yield stresses in pure shear per Eq. (15) are used, one has these four Fourier coefficients as

$$\begin{aligned}
H_0 &= -F_0 + 8F_4 + 4G_4 + \frac{1}{4}\left(\frac{\sigma_0}{\sigma_b}\right)^6 + \frac{1}{8}\left(\frac{\sigma_0}{\sigma_{s0}}\right)^6 + \frac{1}{8}\left(\frac{\sigma_0}{\sigma_{s45}}\right)^6,\\
H_1 &= -3F_1 - 2G_1 + \frac{3}{2}\left(\frac{1-r_b}{1+r_b}\right)\left(\frac{\sigma_f}{\sigma_b}\right)^6,\\
N_0 &= -16F_4 - 2G_0 - 8G_4 + \frac{1}{2}\left(\frac{\sigma_0}{\sigma_b}\right)^6 - \frac{1}{4}\left(\frac{\sigma_0}{\sigma_{s0}}\right)^6 - \frac{1}{4}\left(\frac{\sigma_0}{\sigma_{s45}}\right)^6,\\
N_2 &= 32F_6 - 2G_2 + \frac{1}{4}\left(\frac{\sigma_f}{\sigma_{s45}}\right)^6 - \frac{1}{4}\left(\frac{\sigma_f}{\sigma_{s0}}\right)^6.
\end{aligned} \tag{37}$$

Both the first two biaxial tension yield stresses σ_{p0} and σ_{p45} or the last two biaxial tension yield stresses σ_{p45} and σ_{p90} per Eq. (16) can also be used instead of the two pure shear yield stresses σ_{s0} and σ_{s45} for obtaining the four Fourier coefficients. Their analytical results are rather lengthy and thus omitted here.

It is noted that for typical polycrystalline sheet metals both $r_\theta > 0$ and $r_b > 0$ thus $1+r_\theta > 1$ and $1+r_b > 1$. So they can be used as denominators in the equations given here for uniquely computing the Fourier coefficients.

Appendix C: List of equations for parameter identification using less than twelve uniaxial tensile measurements

Here some examples are given on parameter identification of a sixth-order yield function by considering on-axis and off-axis measurements separately. Instead of using the 16 independent Fourier coefficients, the polynomial material constants ($A_1, \ldots, A_{16}$) of Φ_6 in Eq. (4) are better suited for our purpose here as they are naturally grouped into seven on-axis ones $\boldsymbol{A}_{\text{on}}$=($A_1, \ldots, A_7$) and nine off-axis ones $\boldsymbol{A}_{\text{off}}$=($A_8, \ldots, A_{16}$).

First, the seven on-axis material constants can readily be determined using various choices of seven on-axis measurements. From Eqs. (10)–(16) and the results in "Appendix A," one has the following seven linear equations in terms of $A_1, \ldots, A_7$ for a default set of on-axis measurements (σ_0, r_0, σ_{90}, r_{90}, σ_b, r_b, σ_{p0}):

$$\begin{aligned}
&A_1 = \left(\frac{\sigma_f}{\sigma_0}\right)^6, \quad 6r_0A_1 + (1+r_0)A_2 = 0,\\
&A_7 = \left(\frac{\sigma_f}{\sigma_{90}}\right)^6, \quad (1+r_{90})A_6 + 6r_{90}A_7 = 0,\\
&A_1 + A_2 + A_3 + A_4 + A_5 + A_6 + A_7 = \left(\frac{\sigma_f}{\sigma_b}\right)^6,\\
&6r_bA_1 + (-1+5r_b)A_2 + 2(-1+2r_b)A_3 + 3(-1+r_b)A_4\\
&\quad + 2(-2+r_b)A_5 + (-5+r_b)A_6 - 6A_7 = 0,\\
&64A_1 + 32A_2 + 16A_3 + 8A_4 + 4A_5 + 2A_6 + A_7 = 64\left(\frac{\sigma_f}{\sigma_{p0}}\right)^6.
\end{aligned} \tag{38}$$

They may be written in a matrix form $\boldsymbol{P}\boldsymbol{A}_{\text{on}} = \boldsymbol{Q}$ suitable for numerical calculations

$$\begin{pmatrix} 1 & 0 & 0 & 0 & 0 & 0 & 0 \\ 6r_0 & r_0+1 & 0 & 0 & 0 & 0 & 0 \\ 0 & 0 & 0 & 0 & 0 & 0 & 1 \\ 0 & 0 & 0 & 0 & 0 & r_{90}+1 & 6r_{90} \\ 1 & 1 & 1 & 1 & 1 & 1 & 1 \\ 6r_b & 5r_b-1 & 4r_b-2 & 3r_b-3 & 2r_b-4 & r_b-5 & -6 \\ 64 & 32 & 16 & 8 & 4 & 2 & 1 \end{pmatrix} \begin{pmatrix} A_1 \\ A_2 \\ A_3 \\ A_4 \\ A_5 \\ A_6 \\ A_7 \end{pmatrix} = \begin{pmatrix} \tilde{\sigma}_0^6 \\ 0 \\ \tilde{\sigma}_{90}^6 \\ 0 \\ \tilde{\sigma}_b^6 \\ 0 \\ 64\tilde{\sigma}_{p0}^6 \end{pmatrix}. \tag{39}$$

It is noted that the determinant of the 7-by-7 matrix $\boldsymbol{P}$ above is $4(1+r_0)(1+r_{90})(1+r_b)$. Similarly, a 7-by-7 matrix can also be formed based on other choices of seven on-axis measurements.

For the case of $(\sigma_0, r_0, \sigma_{90}, r_{90}, \sigma_b, r_b, \sigma_{p90})$

$$\boldsymbol{P} = \begin{pmatrix} 1 & 0 & 0 & 0 & 0 & 0 & 0 \\ 6r_0 & r_0+1 & 0 & 0 & 0 & 0 & 0 \\ 0 & 0 & 0 & 0 & 0 & 0 & 1 \\ 0 & 0 & 0 & 0 & 0 & r_{90}+1 & 6r_{90} \\ 1 & 1 & 1 & 1 & 1 & 1 & 1 \\ 6r_b & 5r_b-1 & 4r_b-2 & 3r_b-3 & 2r_b-4 & r_b-5 & -6 \\ 1 & 2 & 4 & 8 & 16 & 32 & 64 \end{pmatrix} \tag{40}$$

where $\boldsymbol{Q} = (\tilde{\sigma}_0^6, 0, \tilde{\sigma}_{90}^6, 0, \tilde{\sigma}_b^6, 0, 64\tilde{\sigma}_{p90}^6)^T$ and $\det\boldsymbol{P} = 4(1+r_0)(1+r_{90})(1+r_b)$.

For the case of $(\sigma_0, r_0, \sigma_{90}, r_{90}, \sigma_b, \sigma_{p0}, \sigma_{p90})$

$$\boldsymbol{P} = \begin{pmatrix} 1 & 0 & 0 & 0 & 0 & 0 & 0 \\ 6r_0 & r_0+1 & 0 & 0 & 0 & 0 & 0 \\ 0 & 0 & 0 & 0 & 0 & 0 & 1 \\ 0 & 0 & 0 & 0 & 0 & r_{90}+1 & 6r_{90} \\ 1 & 1 & 1 & 1 & 1 & 1 & 1 \\ 64 & 32 & 16 & 8 & 4 & 2 & 1 \\ 1 & 2 & 4 & 8 & 16 & 32 & 64 \end{pmatrix} \tag{41}$$

where $\boldsymbol{Q} = (\tilde{\sigma}_0^6, 0, \tilde{\sigma}_{90}^6, 0, \tilde{\sigma}_b^6, 64\tilde{\sigma}_{p0}^6, 64\tilde{\sigma}_{p90}^6)^T$ and $\det\boldsymbol{P} = 48(1+r_0)(1+r_{90})$.

For the case of $(\sigma_0, r_0, \sigma_{90}, r_{90}, r_b, \sigma_{p0}, \sigma_{p90})$

$$\boldsymbol{P} = \begin{pmatrix} 1 & 0 & 0 & 0 & 0 & 0 & 0 \\ 6r_0 & r_0+1 & 0 & 0 & 0 & 0 & 0 \\ 0 & 0 & 0 & 0 & 0 & 0 & 1 \\ 0 & 0 & 0 & 0 & 0 & r_{90}+1 & 6r_{90} \\ 6r_b & 5r_b-1 & 4r_b-2 & 3r_b-3 & 2r_b-4 & r_b-5 & -6 \\ 64 & 32 & 16 & 8 & 4 & 2 & 1 \\ 1 & 2 & 4 & 8 & 16 & 32 & 64 \end{pmatrix} \tag{42}$$

where $\boldsymbol{Q} = (\tilde{\sigma}_0^6, 0, \tilde{\sigma}_{90}^6, 0, 0, 64\tilde{\sigma}_{p0}^6, 64\tilde{\sigma}_{p90}^6)^T$ and $\det\boldsymbol{P} = 144(1+r_0)(1+r_{90})(1-r_b)$. So, when $r_b = 1$, it cannot be used.

For the case $(\sigma_0, r_0, \sigma_{90}, r_{90}, \sigma_b, \sigma_{s0}, \sigma_{p0})$

$$\boldsymbol{P} = \begin{pmatrix} 1 & 0 & 0 & 0 & 0 & 0 & 0 \\ 6r_0 & r_0+1 & 0 & 0 & 0 & 0 & 0 \\ 0 & 0 & 0 & 0 & 0 & 0 & 1 \\ 0 & 0 & 0 & 0 & 0 & r_{90}+1 & 6r_{90} \\ 1 & 1 & 1 & 1 & 1 & 1 & 1 \\ 1 & -1 & 1 & -1 & 1 & -1 & 1 \\ 64 & 32 & 16 & 8 & 4 & 2 & 1 \end{pmatrix} \tag{43}$$

where $\boldsymbol{Q} = (\tilde{\sigma}_0^6, 0, \tilde{\sigma}_{90}^6, 0, \tilde{\sigma}_b^6, \tilde{\sigma}_{s0}^6, 64\tilde{\sigma}_{p0}^6)^T$ and $\det\boldsymbol{P} = -24(1+r_0)(1+r_{90})$.

For the case of $(\sigma_0, \sigma_{90}, \sigma_b, r_b, \sigma_{s0}, \sigma_{p0}, \sigma_{p90})$

$$\boldsymbol{P} = \begin{pmatrix} 1 & 0 & 0 & 0 & 0 & 0 & 0 \\ 0 & 0 & 0 & 0 & 0 & 0 & 1 \\ 1 & 1 & 1 & 1 & 1 & 1 & 1 \\ 6r_b & 5r_b-1 & 4r_b-2 & 3r_b-3 & 2r_b-4 & r_b-5 & -6 \\ 1 & -1 & 1 & -1 & 1 & -1 & 1 \\ 64 & 32 & 16 & 8 & 4 & 2 & 1 \\ 1 & 2 & 4 & 8 & 16 & 32 & 64 \end{pmatrix} \tag{44}$$

where $\boldsymbol{Q} = (\tilde{\sigma}_0^6, \tilde{\sigma}_{90}^6, \tilde{\sigma}_b^6, 0, \tilde{\sigma}_{s0}^6, 64\tilde{\sigma}_{p0}^6, 64\tilde{\sigma}_{p90}^6)^T$ and $\det\boldsymbol{P} = -432(1 + r_b)$.

Next, the nine off-axis material constants can then be determined using various choices of nine independent off-axis measurements. One can set up a set of nine linear equations in terms of $A_8, \ldots, A_{16}$ based on the already known $A_1, \ldots, A_7$ and the nine off-axis measurements such as $(\sigma_{30}, r_{30}, \sigma_{45}, r_{45}, \sigma_{60}, r_{60}, \sigma_{p30}, \sigma_{p45}, \sigma_{p60})$. Other possible choices of the nine off-axis measurements with only two of them from uniaxial tension are $(\sigma_{45}, r_{45}, \sigma_{p15}, \sigma_{p22.5}, \sigma_{p30}, \sigma_{p45}, \sigma_{p60}, \sigma_{p67.5}, \sigma_{p75})$, $(\sigma_{45}, r_{45}, \sigma_{p15}, \sigma_{p30}, \sigma_{p45}, \sigma_{p60}, \sigma_{p75}, \sigma_{s22.5}, \sigma_{s67.5})$, and $(\sigma_{45}, r_{45}, \sigma_{p22.5}, \sigma_{p67.5}, \sigma_{s15}, \sigma_{s30}, \sigma_{s45}, \sigma_{s60}, \sigma_{s75})$, etc. The explicit expressions of the 9-by-9 matrix $\boldsymbol{P}$ in the linear equations $\boldsymbol{P}\boldsymbol{A}_{\text{off}} = \boldsymbol{Q}$ are somewhat lengthy for those cases and are omitted here.

Appendix D: List of equations for parameter identification using limited experimental inputs

Per Sect. 3.2, we subdivide the 16 independent Fourier coefficients into two groups: a set of 12 (F_0, F_1, F_2, F_3, F_4, F_5, F_6, G_0, G_1, G_2, G_3, G_4) to be determined from uniaxial tension measurements and the rest of 4 (H_0, H_1, N_0, N_2) to be determined from biaxial test measurements. The set of those 12 Fourier coefficients is further divided into two subgroups, a set of 7 Fourier coefficients (F_0, F_1, F_2, F_3, F_4, F_5, F_6) related only to the uniaxial yield stresses and a set of 5 Fourier coefficients (G_0, G_1, G_2, G_3, G_4) related also to the uniaxial plastic strain ratios. When there are insufficient experimental inputs, some of those Fourier coefficients associated with higher-order sinusoid terms in the sixth-order yield function ϕ_6 may be set to the values of an isotropic material or some other constants. Linear equations for obtaining the remaining nonzero independent Fourier coefficients are summarized in the following.

(a) ten uniaxial tension measurements (with $F_5 = F_6 = 0$):

$$\begin{pmatrix} F_0 \\ F_1 \\ F_2 \\ F_3 \\ F_4 \end{pmatrix} = \frac{1}{8} \begin{pmatrix} 1 & 2 & 2 & 2 & 1 \\ 2 & 2\sqrt{2} & 0 & -2\sqrt{2} & -2 \\ 2 & 0 & -4 & 0 & 2 \\ 2 & -2\sqrt{2} & 0 & 2\sqrt{2} & -2 \\ 1 & -2 & 2 & -2 & 1 \end{pmatrix} \begin{pmatrix} \tilde{\sigma}_0^6 \\ \tilde{\sigma}_{22.5}^6 \\ \tilde{\sigma}_{45}^6 \\ \tilde{\sigma}_{67.5}^6 \\ \tilde{\sigma}_{90}^6 \end{pmatrix}, \quad \text{or} \tag{45}$$

$$\begin{pmatrix} F_0 \\ F_1 \\ F_2 \\ F_3 \\ F_4 \end{pmatrix} = \frac{1}{12} \begin{pmatrix} 2 & 4 & 0 & 4 & 2 \\ 4 & 4 & 0 & -4 & -4 \\ 3 & 0 & -6 & 0 & 3 \\ 2 & -4 & 0 & 4 & -2 \\ 1 & -4 & 6 & -4 & 1 \end{pmatrix} \begin{pmatrix} \tilde{\sigma}_0^6 \\ \tilde{\sigma}_{30}^6 \\ \tilde{\sigma}_{45}^6 \\ \tilde{\sigma}_{60}^6 \\ \tilde{\sigma}_{90}^6 \end{pmatrix}. \tag{46}$$

The other five Fourier coefficients (G_0, G_1, G_2, G_3, G_4) are to be computed in the same way as given in Eq. (33) and Eq. (35) in "Appendix B" using the corresponding uniaxial tension plastic strain ratios as additional experimental inputs.

(b) eight uniaxial tension measurements (with $F_4 = G_4 = F_5 = F_6 = 0$):

$$\begin{pmatrix} F_0 \\ F_1 \\ F_2 \\ F_3 \end{pmatrix} = \frac{1}{6} \begin{pmatrix} 1 & 2 & 2 & 1 \\ 2 & 2 & -2 & -2 \\ 2 & -2 & -2 & 2 \\ 1 & -2 & 2 & -1 \end{pmatrix} \begin{pmatrix} \tilde{\sigma}_0^6 \\ \tilde{\sigma}_{30}^6 \\ \tilde{\sigma}_{60}^6 \\ \tilde{\sigma}_{90}^6 \end{pmatrix}, \tag{47}$$

$$\begin{pmatrix} G_0 \\ G_1 \\ G_2 \\ G_3 \end{pmatrix} = \frac{1}{6} \begin{pmatrix} 1 & 2 & 2 & 2 \\ 2 & 2 & -2 & -4 \\ 2 & -2 & -2 & 4 \\ 1 & -2 & 2 & -2 \end{pmatrix} \begin{pmatrix} -\frac{6r_0}{1+r_0}(F_0 + F_1 + F_2 + F_3) \\ \frac{3r_{30}}{1+r_{30}}(-2F_0 - F_1 + F_2 + 2F_3) \\ \frac{3r_{60}}{1+r_{60}}(-2F_0 + F_1 + F_2 - 2F_3) \\ \frac{3r_{90}}{1+r_{90}}(-F_0 + F_1 - F_2 + F_3) \end{pmatrix}, \tag{48}$$

or

$$\begin{pmatrix} F_0 \\ F_1 \\ F_2 \\ F_3 \end{pmatrix} = \frac{1}{4} \begin{pmatrix} 1 & 0 & 2 & 1 \\ 1 - \frac{1}{\sqrt{2}} & 2\sqrt{2} & -\sqrt{2} & -1 - \frac{1}{\sqrt{2}} \\ 1 & 0 & -2 & 1 \\ 1 + \frac{1}{\sqrt{2}} & -2\sqrt{2} & \sqrt{2} & -1 + \frac{1}{\sqrt{2}} \end{pmatrix} \begin{pmatrix} \tilde{\sigma}_0^6 \\ \tilde{\sigma}_{22.5}^6 \\ \tilde{\sigma}_{45}^6 \\ \tilde{\sigma}_{90}^6 \end{pmatrix}, \tag{49}$$

$$\begin{pmatrix} G_0 \\ G_1 \\ G_2 \\ G_3 \end{pmatrix} = \frac{1}{6} \begin{pmatrix} 1 & 0 & 4 & 2 \\ 1 - \frac{1}{\sqrt{2}} & 2\sqrt{2} & -2\sqrt{2} & -2 - \sqrt{2} \\ 1 & 0 & -4 & 2 \\ 1 + \frac{1}{\sqrt{2}} & -2\sqrt{2} & 2\sqrt{2} & -2 + \sqrt{2} \end{pmatrix} \begin{pmatrix} -\frac{6r_0}{1+r_0}(F_0 + F_1 + F_2 + F_3) \\ -\frac{3r_{22,5}}{1+r_{22.5}}(2F_0 + \sqrt{2}F_1 - \sqrt{2}F_3) \\ \frac{3r_{45}}{1+r_{45}}(-F_0 + F_2) \\ \frac{3r_{90}}{1+r_{90}}(-F_0 + F_1 - F_2 + F_3) \end{pmatrix}, \tag{50}$$

(c) six uniaxial tension measurements (with $F_3 = G_3 = F_4 = G_4 = F_5 = F_6 = 0$):

$$\begin{pmatrix} F_0 \\ F_1 \\ F_2 \end{pmatrix} = \frac{1}{4} \begin{pmatrix} 1 & 2 & 1 \\ 2 & 0 & -2 \\ 1 & -2 & 1 \end{pmatrix} \begin{pmatrix} \tilde{\sigma}_0^6 \\ \tilde{\sigma}_{45}^6 \\ \tilde{\sigma}_{90}^6 \end{pmatrix}, \tag{51}$$

$$\begin{pmatrix} G_0 \\ G_1 \\ G_2 \end{pmatrix} = \frac{1}{4} \begin{pmatrix} 1 & 4 & 2 \\ 2 & 0 & -4 \\ 1 & -4 & 2 \end{pmatrix} \begin{pmatrix} -\frac{6r_0}{1+r_0}(F_0 + F_1 + F_2) \\ \frac{3r_{45}}{1+r_{45}}(-F_0 + F_2) \\ -\frac{3r_{90}}{1+r_{90}}(F_0 - F_1 + F_2) \end{pmatrix}. \tag{52}$$

(d) four uniaxial tension measurements only (with $F_2 = G_2 = F_3 = G_3 = F_4 = G_4 = F_5 = F_6 = 0$):

$$\begin{aligned} F_0 &= \frac{1}{2}\left(\frac{\sigma_f}{\sigma_0}\right)^6 + \frac{1}{2}\left(\frac{\sigma_f}{\sigma_{90}}\right)^6, \quad F_1 = \frac{1}{2}\left(\frac{\sigma_f}{\sigma_0}\right)^6 - \frac{1}{2}\left(\frac{\sigma_f}{\sigma_{90}}\right)^6, \\ G_0 &= -\frac{3}{(1+r_0)(1+r_{90})}\left[(r_0 + r_0 r_{90} + r_{90})\left(\frac{\sigma_f}{\sigma_0}\right)^6 + r_0 r_{90}\left(\frac{\sigma_f}{\sigma_{90}}\right)^6\right], \\ G_1 &= -\frac{3}{(1+r_0)(1+r_{90})}\left[((r_0 + r_0 r_{90} - r_{90})\left(\frac{\sigma_f}{\sigma_0}\right)^6 - r_0 r_{90}\left(\frac{\sigma_f}{\sigma_{90}}\right)^6\right]. \end{aligned} \tag{53}$$

(e) three on-axis biaxial tension measurements only (with $N_2 = 0$ and up to 12 uniaxial tension measurements):

$$\begin{aligned} H_0 &= -F_0 + 8F_4 - 16F_6 + G_2 + 4G_4 + \frac{1}{4}\left(\frac{\sigma_0}{\sigma_b}\right)^6 + \frac{1}{4}\left(\frac{\sigma_0}{\sigma_{s0}}\right)^6, \\ H_1 &= -3F_1 - 2G_1 + \frac{3}{2}\left(\frac{1-r_b}{1+r_b}\right)\left(\frac{\sigma_f}{\sigma_b}\right)^6, \\ N_0 &= -16F_4 + 32F_6 - 2G_0 - 2G_2 - 8G_4 + \frac{1}{2}\left(\frac{\sigma_0}{\sigma_b}\right)^6 - \frac{1}{2}\left(\frac{\sigma_0}{\sigma_{s0}}\right)^6. \end{aligned} \tag{54}$$

(f) two equal biaxial tension measurements σ_b and r_b (with $N_0 = -7$, $N_2 = 0$):

$$\begin{aligned} H_0 &= \frac{7}{2} - F_0 - G_0 + \frac{1}{2}\left(\frac{\sigma_0}{\sigma_b}\right)^6, \\ H_1 &= -3F_1 - 2G_1 + \frac{3}{2}\left(\frac{1-r_b}{1+r_b}\right)\left(\frac{\sigma_f}{\sigma_b}\right)^6. \end{aligned} \tag{55}$$

(g) one equal biaxial tension measurement σ_b or r_b (with $N_0 = -7$, $H_1 = N_2 = 0$):

$$H_0 = \frac{7}{2} - F_0 - G_0 + \frac{1}{2}\left(\frac{\sigma_0}{\sigma_b}\right)^6, \quad \text{or} \tag{56.1}$$

$$H_0 = \frac{7}{2} - F_0 - G_0 + \left(\frac{1+r_b}{1-r_b}\right)F_1 + \frac{2}{3}\left(\frac{1+r_b}{1-r_b}\right)G_1, \tag{56.2}$$

when $r_b \neq 1$.

References

1. Ahmadi, A., Olshevsky, A., Parrilo, P., Tsitsiklis, J.: NP-hardness of deciding convexity of quartic polynomials and related problems. Math. Progr. Ser. A **137**, 453–476 (2013)
2. Aretz, H., Hopperstad, O.S., Lademo, O.G.: Yield function calibration for orthotropic sheet metals based on uniaxial and plane strain tensile tests. J. Mat. Process. Technol. **186**, 221–235 (2007)
3. Barlat, F., Yoon, J.W., Cazacu, O.: On linear transformations of stress tensors for the description of plastic anisotropy. Int. J. Plast. **23**(3), 876–896 (2007)
4. Carrell, J.B.: Fundamentals of Linear Algebra, pp. 363–364. http://www.math.ubc.ca/~carrell/NB.pdf (2005). Accessed 26 Apr 2017
5. Drucker, D.: Relations of experiments to mathematical theories of plasticity. J. Appl. Mech. **16**, 349–357 (1949)
6. Gotoh, M.: A theory of plastic anisotropy based on a yield function of fourth order (plane stress state)-I. Int. J. Mech. Sci. **19**, 505–512 (1977)
7. Gotoh, M.: A theory of plastic anisotropy based on a yield function of fourth order (plane stress state)-II. Int. J. Mech. Sci. **19**, 513–520 (1977)
8. Hershey, A.: The plasticity of an isotropic aggregate of anisotropic face centred cubic crystals. J. Appl. Mech. Trans. ASME **21**, 241–249 (1954)
9. Hill, R.: A theory of the yielding and plastic flow of anisotropic metals. Proc. R. Soc. Lond. **A193**, 281–297 (1948)
10. Hill, R.: The Mathematical Theory of Plasticity, p. 330. Clarendon Press, Oxford (1950)
11. Hill, R.: Theoretical plasticity of textured aggregates. Math. Proc. Camb. Philos. Soc. **85**, 179–191 (1979)
12. Hill, R.: Basic stress analysis of hyperbolic regimes in plastic media. Math. Proc. Camb. Philos. Soc **88**, 359–369 (1980)
13. Hill, R.: Constitutive modeling of orthotropic plasticity in sheet metals. J. Mech. Phys. Solids **38**, 403–417 (1990)
14. Hosford, W.F.: A generalized isotropic yield criterion. J. Appl. Mech. Trans. ASME **39**, 607–609 (1972)
15. Hosford, W.F.: Comments on anisotropic yield criteria. Int. J. Mech. Sci. **27**, 423–427 (1985)
16. Hosford, W.F.: The Mechanics of Crystals and Textured Polycrystals. Oxford University Press, Oxford (1993)
17. Hu, W.: An orthotropic yield criterion in a 3-D general stress state. Int. J. Plast. **21**, 1771–1796 (2005)
18. Karafillis, A.P., Boyce, M.C.: A general anisotropic yield criterion using bounds and a transformation weighting tensor. J. Mech. Phys. Solids **41**(12), 1859–1886 (1993)
19. Logan, R., Hosford, W.: Upper-bound anisotropic yield locus calculations assuming pencil glide. Int. J. Mech. Sci. **22**, 419–430 (1980)
20. Savoie, J., MacEwen, S.R.: A sixth order inverse potential function for incorporation of crystallographic texture into predictions of properties of aluminum sheet. Textures Microstruct. **26–27**, 495–512 (1996)
21. Soare, S., Barlat, F.: Convex polynomial yield functions. J. Mech. Phys. Solids **58**, 1804–1818 (2010)

22. Soare, S., Yoon, J.W., Cazacu, O.: On the use of homogeneous polynomials to develop anisotropic yield functions with applications to sheet forming. Int. J. Plast. **24**(6), 915–944 (2008)
23. Tong, W.: Application of Gotoh's orthotropic yield function for modeling advanced high-strength steel sheets. ASME J. Manuf. Sci. Eng. **138**, 094502-1–094502-5 (2016)
24. Tong, W.: Generalized fourth-order Hill's 1979 yield function for modeling sheet metals in plane stress. Acta Mech. **227**(10), 2719–2733 (2016)
25. Tong, W.: On the parameter identification of polynomial anisotropic yield functions. ASME J. Manuf. Sci. Eng. **138**, 071002-1–071002-8 (2016)
26. Tong, W., Alharbi, M.: Comparative evaluation of non-associated quadratic and associated quartic plasticity models for orthotropic sheet metals. Int. J. Solids Struct. **128**, 133–148 (2017)
27. Van Houtte, P., Van Bael, A.: Convex plastic potentials of fourth and sixth rank for anisotropic materials. Int. J. Plast. **20**, 1505–1524 (2004)
28. Vegter, H., ten Horn, C., An, Y., Atzema, E., Pijlman, H., den Boogaard, T., Huetink, H.: Characterization and modelling of plastic material behaviour and its application in sheet metal forming simulation. In: Onate, E., Owen, D.R.J. (eds.) Proceedings of VII International Conference on Plasticity. Barcelona (2003)
29. Yang, W.: A useful theorem for constructing convex yield function. J. Appl. Mech. ASME **47**, 301–303 (1980)
30. Yoshida, F., Hamasaki, H., Uemori, T.: A user-friendly 3D yield function to describe anisotropy of steel sheets. Int. J. Plast. **45**, 119–139 (2013)
31. Yoshida, F., Hamasaki, H., Uemori, T.: Modeling of anisotropic hardening of sheet metals including description of the Bauschinger effect. Int. J. Plast. **75**, 170–188 (2015)
32. Zhou, Y., Jonas, J., Savoie, J., Makinde, A., MacEwen, S.: Effect of texture on earing in FCC metals: finite element simulations. Int. J. Plast. **14**(1–3), 117–138 (1998)